USGS
science for a changing world

U.S. DEPARTMENT OF THE INTERIOR
U.S. GEOLOGICAL SURVEY

PRELIMINARY SCIENTIFIC RESULTS OF THE CREEDE CALDERA CONTINENTAL SCIENTIFIC DRILLING PROGRAM

P.M. Bethke, Editor

Open-File Report 94-260-M

2001

ROCK MAGNETIC STUDIES OF THE OLIGOCENE CREEDE FORMATION AND PROSPECTS FOR A POLARITY STRATIGRAPHY

By

R.L. Reynolds
J.G Rosenbaum
D.S. Sweetkind
U.S. Geological Survey, Denver CO
M.A. Lanphere
U.S.Geological Survey, MS Menlo Park, CA
C.A. Rice
M.L. Tuttle
U.S. Geological Survey, Denver CO

ABSTRACT

Sedimentary and volcaniclastic rocks of the Oligocene Creede Formation fill the moat of the Creede caldera, which formed about 26.89 Ma during the eruption of the Snowshoe Mountain Tuff. Paleomagnetic and rock magnetic studies of two cores (418 and 703 m-long) that penetrated the lower half of the Creede Formation provide information on the age of the caldera fill and on postdepositional alteration, which has obscured the polarity stratigraphy. The age and duration of sedimentation of the Creede Formation are constrained by $^{40}Ar/^{39}Ar$ ages on the Snowshoe Mountain Tuff (26.89±0.05 Ma) and on lava flows of the Fisher Quartz Latite (26.23±0.05 Ma) that overlie the Creede Formation.

In both cores, volcanic breccia, graded tuffs, and fluvial deposits having high magnetic susceptibility (MS; typically $>10^{-2}$ volume SI) are overlain by mostly finer-grained lacustrine beds and tuffs having generally lower MS (typically $<2.5x10^{-4}$). The transition between high and low MS occurs over an interval of less than 30 m and corresponds more closely to a geochemical boundary than to a facies change. The geochemical boundary separates a deep zone with sparse pyrite from a shallow sulfidized zone with locally abundant pyrite. In the sulfidized zone, much of the pyrite formed at the expense of detrital titanomagnetite.

Our paleomagnetic study, which focuses on volcanic deposits and some immediately underlying and overlying lacustrine beds, yields an ambiguous polarity zonation. Normal polarity magnetizations are found in Snowshoe Mountain Tuff beneath the moat sediments, in detrital-magnetite-bearing graded tuffs in the high MS zone, and in a bed of air-fall ash from outcrop about 200 m stratigraphically above the top of core 2. Normal polarity also characterizes most core samples from detrital-magnetite-bearing tuff and sandstone beds that escaped severe alteration in the sulfidized zone and that have natural remanent magnetization magnitudes greater than 10^{-2} A/m. More weakly magnetized rocks in the sulfidized zones have either normal or reversed polarity that are carried by magnetite and (or) maghemite. Many more reversals are found than can be accommodated by any geomagnetic polarity time scale over the interval between the ages of the bounding extrusive units. Moreover, several polarity changes are recorded by specimens separated by only a few centimeters without intervening hiatuses and by specimens in several tuff beds, each of which represents a single depositional event. These polarity changes thus cannot be attributed to detrital remanent magnetization. Many polarity changes are apparently related to chemical remanent magnetization carried by post-depositional magnetite and maghemite that formed in rocks in which most or all detrital iron oxide was destroyed. Incipient oxidation of pyrite may have produced the secondary iron oxides, but such an origin has not been confirmed.

INTRODUCTION

Rock magnetic and paleomagnetic studies of the Creede caldera moat cores (figs. 1 and 2) are underway to help (1) correlate between cores; (2) estimate the time span represented by the moat fill; and (3) understand the conditions and timing of post-depositional alteration. The two cores were drilled to investigate the depositional, structural, and geochemical settings of the intracaldera fill and to test theories on the fluid and geochemical links between the moat sedimentary fill and the Creede epithermal vein system. The geologic setting and goals of the project are summarized by Bethke and Lipman (1987); Bethke (1994) and Campbell (1993). The core material is described by Hulen (1992). In this paper, we follow the stratigraphic nomenclature of Larsen and Crossey (1994) and Larsen and Nelson (1999) who present the general stratigraphy of the cores and the geophysical properties of the boreholes.

We have focussed primarily on studies of magnetic susceptibility, magnetic-mineral alteration, and paleomagnetism of pyroclastic rocks. In this report, we present some preliminary results on the polarity stratigraphy, which has proved to be a sticky problem. In particular, we discuss the following rock magnetic, paleomagnetic, petrologic, and chemical results that bear on correlations and on the depositional mechanisms, duration of moat filling, and alteration of the caldera moat fill:

1. Magnetic susceptibility as a basis for correlations between cores and as a guide for studies of alteration;
2. petrographic observations and preliminary sulfur and organic carbon geochemical data that help reveal the effects of sulfidization on magnetic properties;
3. certain magnetic properties, mainly magnitude of natural remanent magnetization (NRM), that in conjunction with alteration studies may help evaluate the reliability of paleomagnetic results;
4. remanent magnetizations of the ash-flow tuff at the bottom of core 2;
5. remanent magnetizations of breccias and conglomerates that constrain depositional mechanisms of these coarse-grained facies--whether emplaced as hot or cold deposits--and to evaluate their use for polarity stratigraphy.
6. remanent magnetizations of fine-grained, lacustrine facies--especially air-fall tuff beds but also some enveloping sandstone and siltstone beds--that contribute to the polarity stratigraphy.

We also present preliminary paleomagnetic results from a bed of air-fall ash in outcrop, about 3 km northwest of core 2 (site CFA-1; Fig. 1). When complementary rock magnetic studies are completed, results from this site will provide a polarity determination at a horizon about one-third up the stratigraphic interval from the top of core 2 to the top of the Creede Formation.

GEOCHRONOMETRIC CONSTRAINTS ON THE AGE AND DURATION OF SEDIMENTATION

A magnetic polarity stratigraphy may contain a detailed temporal record of sedimentation, if the magnetizations were acquired at or very shortly after deposition and in the absence of major hiatuses (e.g., Jacobs, 1984). Any such record must be compatible with any available geochronometric framework, which in this study is provided by $^{40}Ar/^{39}Ar$ isotopic dates on the underlying Snowshoe Mountain Tuff and on two lava flows of the Fisher Quartz Latite that overlie the moat sedimentary rocks (Lanphere, 1994).

An age of 26.89±0.05 Ma was obtained for the Snowshoe Mountain Tuff using biotite in samples from core 2 and from outflow tuff at Cattle Mountain. An age of 26.23±0.05 Ma for the Fisher flows represents a pooled age from a locality on Fisher Mountain and from one on Copper Mountain. The ages were determined using SB-3 biotite as the flux monitor mineral (age of 162.9±1.3 Ma) using techniques described by Dalrymple and Lanphere (1971, 1974), Dalrymple et al. (1981), and Lanphere (1988; 1994). Considering the ages and their uncertainties, the deposition of the Creede Formation probably occurred over a period of about 600,000 to 700,000 years. Most of this period would be represented by normal polarity on the basis of a comparison of the age results with the geomagnetic polarity time scale of Harland et al. (1990) (fig. 3). Analytical uncertainty would allow for either normal or reversed polarity near the top of the Creede Formation. The Snowshoe Mountain Tuff and all three sampled flows of the Fisher Quartz Latite have normal polarity magnetizations (Rosenbaum, et al., 1987; Tanaka and Kono, 1973; Beck et al., 1977).

METHODS

Magnetic susceptibility (MS) was measured on whole-core segments at 1-foot (about 0.3 m) intervals by passing the core through a 11.6-cm-diameter coil. Measurements were made at 600 Hz in a field of 0.1 millitesla (mT) using a Sapphire Instruments SI-2 susceptometer that was calibrated using plexiglass cylinders filled with MnO_2. In the laboratory MS of standard paleomagnetic specimens (volume about 10 cm^3), as well as disaggregated and powdered samples, was measured by the same susceptometer with a smaller (3-cm diameter) coil (table 1).

Paleomagnetic measurements of core samples, which were oriented vertically, but not azimuthally, were made using a cryogenic magnetometer, a 5-Hz Schonstedt DSM-1 spinner magnetometer, or a 90-Hz Geofysika JR5 spinner magnetometer. Directions of remanent magnetization (table 1) were determined by least-squares line fitting of demagnetization decay paths (Zijderveld, 1967; Kirschvink, 1980). Each sample was demagnetized either in progressive alternating-fields (AF), typically in 10 steps from 5 mT to 80 mT peak induction, or by thermal techniques, typically in 8 steps from 100 °C to 600 °C. Important information on the identity of magnetic minerals can be found in demagnetization results--in the temperatures

over which the magnetization was removed as well as in remanence decay as a function of alternating fields.

To facilitate the analysis and discussion of the paleomagnetic results from the cores, we assigned a "quality rating" to each magnetization decay path (fig. 4): The highest rating of 1 was reserved for results in which the demagnetization path showed nearly straight-line decay to the origin. A rating of 2 was assigned to paths that were curved or kinked and that trended generally toward the origin but that clearly defined a positive or negative inclination. We put little faith in a quality-3 result, which may show a cluster of points at either inclination sign but without clearly defined decay to the origin. Less than 5% of the more than 230 specimens analyzed gave completely erratic results and were eliminated from further analysis.

Another factor to consider in the evaluation of the paleomagnetic data is the magnitude of NRM. Not surprisingly, the NRM magnitude and quality of the demagnetization path are commonly correlated. Below we refer to magnetizations as strong (those having NRM magnitude > 10^{-2} A/m [10^{-5} emu/cc]), moderately strong (NRM magnitude between $2x10^{-3}$ and 10^{-2} A/m), or weak (NRM < $2x10^{-3}$ A/m). In the discussion below we make use of the concept of quality and NRM magnitude in assessing the reliability of the paleomagnetic directions.

Other methods for identifying magnetic minerals include thermomagnetic analysis and direct petrographic observation. Thermomagnetic analysis--the measurement of magnetization as a function of temperature--was used to identify magnetic minerals by measurement of their Curie temperatures. Magnetic iron oxide and iron sulfide minerals have diagnostic Curie temperatures and characteristic shapes of the thermomagnetic curve.

Iron oxide and iron sulfide minerals were also studied using standard reflected-light microscopy at magnifications to about 500x. We examined 51 polished thin sections made from the end pieces of paleomagnetic samples and 10 polished mounts of grains separated magnetically from similar pieces.

Contents of total sulfur and organic carbon were determined by induction furnace (LECO) methods to examine relations among magnetic and chemical properties. Organic carbon was measured after carbonate carbon was removed using dilute HCl. Paleomagnetic specimens, crushed after completion of magnetic measurements, as well as previously disaggregated rocks, were analyzed chemically (table 2).

MAGNETIC SUSCEPTIBILITY OF WHOLE CORES

The magnetic susceptibility-depth profiles for cores 1 and 2 are similar in shape and magnitude, both in gross pattern and in their detail. In the broadest sense, both cores are characterized by high-MS (typically >10^{-2} volume SI) in their lower parts, by mostly uniform and low MS (typically <$2.5x10^{-4}$) in their upper parts, and by an abrupt change from high to low MS over an interval of only about 100 ft (30 m) (fig. 5). The zones of high and low MS correspond crudely to the high-energy, coarse-

grained facies and to the low-energy, fine-grained depositional facies, respectively. That is, rocks in the high MS zone are dominantly tuff breccia, conglomerate, and fluvial sandstone, whereas rocks in the low-MS zone are dominantly laminated beds of silty reworked tuff with intervening beds of air-fall tuff. The boundary between the two MS zones, however, does not correspond exactly to the lithologic boundary that separates the two facies. The MS break occurs, rather, within the coarse-grained rocks (figs. 2 and 5), and it corresponds more closely to a geochemical boundary than to a depositional one. In core 1, the MS break occurs in an interval of interbedded pebble to cobble conglomerate and pebbly sandstone, whereas in core 2 the break occurs within a thick zone of monomictic breccia. As discussed below, the geochemical boundary separates a less altered zone in the lower approximately one-third of the cores from a more altered zone in the upper part that is characterized by pyritic replacement of detrital magnetite.

MAGNETIC SUSCEPTIBILITY AND LITHOLOGY

In both MS zones, high-frequency variations in MS can in many instances be related directly to lithology. Some important observations of the lithologic control on MS are described below:

1. Welded Snowshoe Mountain Tuff in the bottom 191 ft (58 m) of core 2 has nearly uniform and high MS ($>2.5 \times 10^{-2}$), except for much lower MS at the bottom of the core in the 10-ft (≈3-m) thick zone of intense pyritic and calcitic veining. MS is noticeably diminished even in zones of lesser veining. An approximately 60 ft (18 m) interval of tuffaceous breccia at the base of core 1, tentatively identified as non-welded ash-flow tuff (Hulen, 1992), has MS values lower by a factor of 2 than the welded ash-flow tuff in core 2.

2. Strongly graded ash-fall tuff beds, the A tuffs of Larsen and Nelson (1999), exhibit similarly large variations in MS with changes in grain size. The bottom 20 ft of the graded tuff in both cores (GT, fig. 5) have identical values of MS, and both tuffs show an upward decrease in MS with a decrease in grain size that accompanies an increase in the degree of sorting (Larsen and Nelson, 1999). The relative abundance of detrital magnetite in the coarser-grained, more poorly sorted basal parts reflects a high energy of sediment transport, perhaps in the ash cloud during the initial stages of eruption. Sorting, either in the eruption column or by post-depositional reworking, progressively removed at least some of the heavy Fe-Ti oxide minerals. These MS patterns in the A tuffs strongly corroborate the proposed correlation of the tuff beds by Larsen and Nelson (1999) made on the basis of mineralogy and geophysical properties.

3. Many of the air-fall tuffs in the altered zone show more variation in MS than do surrounding rocks. Over most of their vertical thickness, the tuffs have lower

MS than surrounding rocks. The basal parts of some tuffs, however, have MS values as high as, or higher than, the average value for the subjacent and superjacent beds (G and E tuffs; core 2; fig. 6 a, b; Larsen and Nelson, 1999). The high MS diminishes upward, perhaps a result of increased sorting. In some tuffs (for example, E and G tuffs) upward decreases in MS are interrupted by abrupt increases in MS, possibly indicating a renewed pulse of air-fall ash and an accompanying reversal in sorting. Such MS features, either strongly or subtly expressed, not only contribute to our understanding of the depositional processes but may also have value for correlation. In this respect, some remarkable similarities can be seen in tuffs from the two cores. For example, the G tuffs in both cores have identical MS values in the bottom 4 ft, and show the same pattern of MS variation upward, with at least one, and perhaps two increases in MS superimposed on an overall decrease in MS (Fig. 6 a).

4. Relatively coarse-grained beds or pyroclastic deposits, other than the bottoms of some air-fall tuff beds, in the high-sulfur, low-MS zone commonly have higher MS than surrounding laminated siltstone (Fig. 5) Some examples are conglomeratic sub-lacustrine debris-flow strata in core 1 between 130 and 285 ft; pumiceous breccia in core 2 between 1020 and 1030 ft. These observations are important for a future paleomagnetic strategy as discussed below.

GEOCHEMICAL RESULTS, MAGNETIC MINERALOGY, AND PETROGRAPHIC OBSERVATIONS BEARING ON POST-DEPOSITIONAL ALTERATION

Post-depositional alteration, particularly sulfidization as expressed by the formation of pyrite at the expense of detrital magnetic iron-titanium (Fe-Ti) oxide minerals, has strongly affected the magnetic properties of much of the Creede Formation. Thus, it is important to consider the paleomagnetic results in light of preliminary geochemical data and petrographic observations of sulfidic alteration.

Pyrite occurs through both cores, including in the Snowshoe Mountain Tuff at the bottom of core 2, but it is abundant only in the low MS zone. In this zone at least much of the pyrite is a diagenetic product of bacterial sulfate reduction (McKibben and Eldridge, 1994). The primary source of the sulfur was probably sulfate aerosols in eruption columns. Detrital organic debris carried into the lake and organic matter that grew in the lake probably provided food sources for the sulfate-reducing bacteria.

The relations among sulfur and MS illustrate the effects of sulfidization on magnetic properties (Fig. 7). MS values show strong inverse relation to total sulfur content: high MS corresponds to low sulfur, whereas low MS corresponds to high sulfur contents regardless of lithology.

Another, but less direct, indicator of pyrite comes from MS measurements of thermally demagnetized samples; MS was measured on most samples after each

demagnetization step. The original presence of pyrite in many samples is indicated by strong increases in MS, because heating above about 400 to 450 °C causes the alteration of pyrite to magnetite, as well as to maghemite and hematite.

Petrographic observations show clearly the effect of sulfidization on detrital titanium-bearing magnetite. The most common sulfide-oxide mineral association is the presence of pyrite rims around magnetite or around former titanium-bearing magnetite grains, the magnetite having been destroyed by complete leaching of iron. In these latter cases, the original presence of Ti-magnetite is indicated by remnants of ilmenite, or by TiO_2 formed from ilmenite, as lamellae in {111} crystallographic orientation. Occurrences of pyrite rims around former magnetite, now leached of its iron, is a common expression of sulfidization in which H_2S causes diffusion of iron from the iron oxide (Canfield and Berner, 1987). Many former oxide grains display an outer rim of pyrite that replaced the magnetite; rarely, entire magnetite grains have been fully replaced by pyrite.

In some sections, we could find no magnetite, even though thermal demagnetization results indicated unblocking temperatures diagnostic for magnetite, as discussed below. In other sections, generally from coarse-grained rocks, small relicts of formerly large magnetite grains remain inside thick rims of pyrite. In some of the samples devoid of magnetite, ferrimagnetic ferrian ilmenite is present. Such ferrian ilmenite was identified in polished grain mounts of magnetic-mineral separates and by thermomagnetic analysis (fig. 8). The resistance of ferrian ilmenite, and other varieties of the ilmenite-hematite solid solution series, to sulfidization has been documented (see Reynolds, 1982; Dimanche and Bartholomé, 1976). These grains are optically homogeneous, their rapid cooling in volcanic rocks having prevented exsolution into separate phases.

It is perhaps important to this study that ferrian ilmenite of certain compositional range ($0.45<x<0.60$, for $Fe(III)_{2-2x}\ Fe(II)\ Ti_x\ O_3$) has an unusual capacity for self-reversal of magnetization. That is, the minerals may acquire a stable remanent magnetization when cooled from elevated temperatures ($>\approx 200$ °C) in a direction opposite to that of the applied field (see Hoffman, 1975). One thermomagnetic analysis of a magnetic extract of ferrian ilmenite (501.5 ft in core 1) gave a Curie temperature of 110 °C (fig. 8), corresponding to a composition of $x\approx 0.5$, which is well within the self-reversing range.

PALEOMAGNETISM

Establishment of a polarity stratigraphy

At the outset we expected that attempts to establish a polarity stratigraphy would depend on different rock types that have different types of remanent magnetization. Welded ash-flow tuffs, for example, acquire thermoremanent magnetization (TRM) when certain contained Fe-Ti oxide minerals, predominantly magnetite, cool below their Curie temperatures. If emplaced at elevated temperatures as hot lahars, even at temperatures less than Curie temperatures, volcanic breccias and conglomerates

may similarly acquire a partial TRM (PTRM) in the direction of the ambient magnetic field (Hoblitt and Kellogg, 1979). By contrast, remanent magnetization in breccia and conglomerate deposited at low temperature would be approximately random, in the absence of later magnetic overprints, because the geomagnetic field is too weak to align physically large rock fragments. Finer grained pyroclastic deposits such as reworked air-fall tuffs, as well as sandstone and siltstone, commonly acquire a depositional remanent magnetization (DRM) parallel, or approximately so, to the ambient magnetic field by the alignment of individual detrital magnetic particles.

Post-depositional alteration, however, can affect any type of primary or earlier remanent magnetization, either by the destruction of original magnetic grains or by the chemical growth of new ones. Such growth can generate a chemical remanent magnetization (CRM) that may obscure or overwhelm the original remanence, especially if primary grains have been destroyed.

Another type of secondary or overprint remanent magnetization that might complicate a polarity stratigraphy in borehole core is isothermal remanent magnetization (IRM). IRM is acquired in a steady, generally strong, field that can be associated with the magnetization of drill strings. We expect that during drilling such magnetization is directed steeply downward, nearly parallel to the drill string. Only the large, low-coercivity (magnetically "soft") magnetic grains, such as multidomain magnetite, would be adversely affected, and even then, demagnetization treatment can often remove the effects.

Paleomagnetism of ash-flow tuff, core 2

Paleomagnetic behavior of the ash-flow tuff in core 2 is easily interpreted and defines a normal polarity. All 13 specimens showed moderate-coercivity, single-component magnetizations that, together with petrographic examination, imply a thermoremanent magnetization (TRM) carried by primary magnetite. The in-situ mean inclination calculated by the method of McFadden and Reid (1982) is 74.2°, α_{95}=2.8°. Because of the 5° offset in the borehole attitude (Nelson and Kibler, 1994), the corrected mean inclination represents a range of possible inclinations as illustrated in figure 9. The paleomagnetic results are fully consistent with chemical and petrographic results that confirm the basal ash-flow unit in core 2 as Snowshoe Mountain Tuff (Lipman and Weston, 1994).

Paleomagnetism of breccia and conglomerate

One target of paleomagnetic analysis was the tuffaceous, matrix-supported breccia in the bottom ≈60 ft (18 m) of core 1 that might represent either a debris-flow deposit or a lithic-rich, non-welded ash-flow tuff (Hulen, 1992; Larsen and Nelson, 1999). The large scatter in paleomagnetic inclinations, including both positive and negative values (fig. 10), precludes any possibility that this unit acquired a TRM or PTRM. The scatter in remanent inclinations probably represents instead the deposition of clasts in a cold debris flow. Similarly, polymictic tuff breccia (from

depths of 2040-2130 ft and 1860-1950 ft) as well as monomictic tuff breccia (≈1600-1800 ft) in core 2 possess shallow to steep, positive and negative inclination angles (fig. 10) that reflect apparently random orientation of individual clasts. No consistent pattern was evident when comparing nearly adjacent samples of lithic clast and matrix.

Near the top of core 1, we sampled three zones of conglomerate (130-168 ft, 181-184 ft; and 253-284 ft) which we refer to informally as conglomerates 1, 2, and 3, respectively (fig. 2). MS is high (typically greater than $6x10^{-4}$), and spikes of relatively high MS near the upper and lower boundaries of conglomerate 1 resemble MS patterns related to cooling in other volcanic rocks. The upper two conglomerates possess mixtures of positive and negative inclination and thus show no evidence for the acquisition of coherent remanence, whether TRM, PTRM, CRM, or IRM. In conglomerate and coarse-grained sandstone of the conglomerate 3 interval, seven of 12 specimens possess moderate-angle (≈35°-70°) positive inclinations. One specimen had a shallow (18°) positive inclination, two specimens had nearly flat inclinations, and two others had negative inclinations. The predominance of specimens having positive-inclination directions suggests the possibility of a high-temperature origin and thus a reliable TRM. A pervasive normal IRM can be ruled out because of the lack of uniform behavior in nearby specimens and the lack of very steep inclinations.

Paleomagnetism of air-fall tuff and lacustrine beds

Within the breccias in the lower parts of both cores, reworked, graded air-fall tuff beds (A tuff of Larsen and Nelson, 1999) possess normal polarity magnetization. Of 17 samples from the graded tuff doublet in core 1, 16 have well defined moderate to steep (as much as 88°) inclination angles (fig. 11). The trend seen in the inclination, from steep at the bottom to shallower values toward the top of each set, suggests an IRM overprint on the coarse-grained tuff at the base. The simplest explanation for the sole negative inclination is that a core segment or specimen was inadvertently flipped during handling and marking. Results from the graded tuff in core 2 do not show the trend in inclination change with grain size; the average inclination from the method of McFadden and Reid (1982) method is 62.9° (α_{95}=4.1°).

The air-fall tuffs, reworked tuffs, siltstone, and sandstone in the high-sulfur, low-MS zone show predominately moderate to steep, positive or negative inclinations. No obvious polarity zonation has emerged: normal and reversed samples alternate through both cores 1 and 2 (fig. 12).

Many polarity changes occur over short stratigraphic distances or within the same bed. Different polarities are found in specimens separated stratigraphically by only a few centimeters and within the same core segment. Some such changes are found within individual tuff beds, each of which represents a single depositional event (fig. 13). Some specimens even contain both polarities that are recognized at different ranges of unblocking temperatures. A typical example (fig. 14) shows the

removal of positive inclination direction over low temperatures (100 ^{o}C to about 400 ^{o}C) and the isolation at higher temperatures of moderate negative inclination direction. In these samples, as well as in other thermally demagnetized samples that have single-component magnetization, the unblocking temperatures strongly suggest that magnetite, not hematite or pyrrhotite, carries the remanence. The two-component magnetizations have no unique interpretation, and we cannot distinguish among several possibilities: (1) a primary direction (N or R; low- or high-unblocking temperature) with a superimposed secondary magnetization (R or N; high- or low-unblocking temperature); (2) two secondary magnetizations; (3) a primary or secondary reversed magnetization unblocked at the higher temperature range, with a superimposed normal IRM related to core drilling that affected only multidomain magnetite.

The broader pattern of polarities, ill-defined as it is, shows a poor correspondence between the two cores, both in an overall sense and in detailed comparison of presumably equivalent tuffs (fig. 13). Most samples in core 1, from tuff G down to the top of the high-MS zone, have normal polarity, whereas most in core 2 over this interval have reversed polarity. Furthermore, more normal than reversed polarity directions are found in tuffs E and F in core 1, but the opposite is found in those tuffs in core 2 (fig. 13).

The polarity patterns and relations are similar regardless of demagnetization technique. Although many fewer samples were demagnetized by thermal than by AF techniques, the proportion of normal and reversed directions is about the same after the different treatments.

Screening the results on the basis of NRM magnitude, however, reveals a predominance of normal directions (fig. 15). Such a screen, using the arbitrary cut-off of 10^{-2} A/m, eliminates about 80% of all results from core 1 and about 66% of those from core 2. Nearly all reversed directions are dropped from core 1. Of the quality-1 and -2 results in core 2, only two reversed directions survive, compared to 11 normal directions.

Paleomagnetism of air-fall ash, outcrop site CFA-1

The elevation of site CFA-1 is about 2790 m, 160 m above the top of the core 2. No known structural offsets cross the essentially flat-lying Creede Formation between core 2 and site CFA-1. The bed thus allows for a polarity determination at a horizon roughly 200 m stratigraphically above the uppermost sampled interval in drillhole 2 (see Table 1).

AF demagnetization (8 or 9 steps to 60 mT) of six oriented hand samples were analyzed by least-squares line-fits of decay paths on orthogonal demagnetization diagrams. The results (fig. 16) yield a mean direction at D=349.8^{o}; I=68.2^{o}; α_{95}=15.7^{o}; kappa=19.2. Three demagnetization diagrams (fig. 16 b, c, d) illustrate the range of demagnetization behavior, from well defined normal directions (fig. 16 c) to more poorly defined normal directions for weakly magnetized specimens (fig. 16 d). The air-fall ash bed shows no macroscopic evidence of detrimental alteration, related

either to sulfidization or oxidation. The results are tentatively interpreted as normal polarity, pending future studies of the type and origin of the magnetic minerals that carry the remanence.

PROSPECTS FOR A USEFUL POLARITY STRATIGRAPHY

Results from the graded tuffs (A tuff of Larsen and Nelson, 1999) in the low-sulfur, high-MS zone indicate that the lower parts of the Creede Formation have primary normal polarity. A conglomerate bed in the upper part of core 1 has a mostly coherent normal direction that is perhaps a TRM or PTRM acquired during cooling of a debris flow emplaced at elevated temperatures. Results from the air-fall ash bed in outcrop strongly suggests normal polarity at a horizon about one-third up the interval between the top of core 2 and the top of the Creede Formation.

For several reasons, the many polarity changes in the high-sulfur, low-MS zone cannot be attributed to a detrital remanent magnetization (DRM) that recorded the geomagnetic polarity. First, many more reversals are found than can be accommodated by any geomagnetic polarity time scale over the interval between the ages of the bounding extrusive units (fig. 3). Second, several polarity changes are recorded by specimens separated by only a few centimeters without intervening hiatuses. Third, several individual tuff beds, each of which represents a single depositional event, contain apparent reversals. Finally, a different polarity dominates the roughly equivalent parts of the two cores--normal for core 1, reversed for core 2.

A remaining problem is to identify the mineralogic sources and the chemical and (or) physical processes that led to mixed polarities. For reasons detailed below, we tentatively conclude that different degrees of chemical alteration and remagnetization are responsible for most, if not all, of the complex polarity results. If we could recognize the secondary phases and their diagnostic characteristics, or if we could recognize characteristics of DRM in these beds, we could then probably distinguish between reliable and unreliable results. It is likely that a few results come from misoriented paleomagnetic specimens or from samples taken from flipped core segments. Thus, any explanation for mixed polarities must account for most, but not necessarily all, results.

Clues to the paleomagnetic reliability of the sedimentary rocks, other than breccia and conglomerate, are found in observed relations among NRM magnitude, bulk grain size, and polarity. The relatively higher NRM magnitudes ($>10^{-2}$ A/m; $>10^{-5}$ emu/cc) correspond dominantly to normal polarity (table 1). Nearly all such specimens from the low-MS zone represent relatively large bulk sediment grain size, typically larger than fine sand size (table 1). An example of these relations includes an air-fall tuff bed and fine- to medium-grained sandstones directly beneath the tuff (in core 1, about 472 to 504 feet; tuff G of Larsen and Nelson, 1999). In this case the underlying sandstone has strong, normal magnetization. The coarse-grained lower part of the graded tuff also has normal polarity and higher

NRM magnitude than does the interior part of the tuff. The samples having relatively stronger magnetizations contain relict detrital magnetite.

These observations led us to suspect that the coarser-grained rocks are more likely to have detrital magnetite that survived sulfidization than the fine-grained rocks and that the coarse beds consequently are more likely to yield a reliable polarity. This suggestion is paradoxical, because fine-grained sediments are known, in the absence of alteration, to give more reliable paleomagnetic results than do coarse-grained sediments. A combination of small magnetic particles and the generally quiet-water environment that characterize mudstones, for example, are more conducive to efficient magnetic alignment than are larger grains found in sandstone that may represent a high-energy depositional environment. In the highly altered Creede Formation, however, we suggest that the smaller magnetite grains in the fine-grained rocks were removed completely, or nearly so, by sulfidization. Very small amounts of secondary magnetic minerals account for the measurable but weak CRM magnetizations. In contrast, many large magnetite grains had sufficient volume to withstand complete dissolution. Their initial alignment in the geomagnetic field may have been crude, but it was presumably sufficient in many samples for recording the polarity.

We have begun to test the suggestion that relatively coarse-grained beds may have DRM that is reliable with respect to polarity. Paleomagnetic measurements have been completed on specimens of sandstone from the upper 1000 feet of core 2 that have high MS values and that thus may contain preserved detrital magnetite. Seven quality-1 and -2 results in this interval pass the NRM magnitude screen at 10^{-2} A/m, and of these, six have normal polarity. Polished thin sections remain to be examined for magnetic mineralogy.

Currently, we have no evidence that minerals other than magnetite and (or) maghemite are responsible for the inferred chemical remanent magnetization (CRM). The magnetic iron sulfide minerals, pyrrhotite and greigite, have not been implicated by results of thermal demagnetization or of thermomagnetic and petrographic analysis of magnetic and chemical separates. Hematite is similarly precluded as a widespread carrier of CRM.

The role of ferrimagnetic ferrian ilmenite, having compositions within the self-reversing range, as a cause for some apparent reversals is uncertain. As an individual detrital mineral, it would behave as does magnetite, but with a smaller magnetic moment, so that it could align in the ambient field direction. We can think of one way, however, by which a combination of depositional and chemical factors and events could have led to a direction carried by detrital, self-reversing ferrian ilmenite opposite to that of the geomagnetic field at the time of deposition: (1) Ferrian ilmenite occurred in small (sand size or smaller) igneous rock fragments along with dominant magnetite; (2) the TRM directions of the magnetite and ferrian ilmenite were opposite; (3) the fragments were aligned along the magnetic field direction upon deposition according to the magnetization of the magnetite; and finally (4) sulfidization removed all the magnetite, leaving a remanence carried by

ferrian ilmenite in the direction opposite to the original applied field direction at the time of deposition. In magnetic mineral separates, we have observed clasts that contain ilmenite, presumably the ferrimagnetic variety, and grains of altered titanomagnetite in which all Fe has been apparently removed; relicts of magnetite were not seen. The above scenario, thus, seems plausible on the basis of available petrographic and thermomagnetic analyses, but we have not found supporting evidence from thermal demagnetization results.

The origin of the inferred secondary magnetite or maghemite is uncertain. Incipient oxidation of pyrite may have produced the secondary iron oxides, but such an origin has not been confirmed petrographically.

We are left with the question: What polarity results can we trust and how can we improve the sparse polarity record obtained so far? The normal directions from the graded tuff (graded tuff A of Larsen, 1999) in the lower parts of both cores and from the air-fall ash bed in outcrop in the upper part of the Creede Formation provide the most reliable polarity data obtained to date from the Creede Formation. The normal polarities of the Snowshoe Mountain Tuff and of the few sites in Fisher flows provide additional magnetostratigraphic constraints. Most results from strongly magnetized samples from the lacustrine facies indicate a normal polarity that may be related to a relatively high content of preserved detrital magnetite. This possibility requires additional petrographic study. Another approach will be to measure remanent directions of Fisher flows that have been interpreted to interfinger the Creede Formation on the basis of outcrop relations (Steven and Ratté, 1973; Steven and Lipman, 1973; Tom Steven, personal comm., 1994).

SUMMARY

Correlation between the two cores and estimates of the duration of Creede Formation sedimentation based on paleomagnetic polarity require the presence of an original TRM or DRM. We have observed, however, that sulfidization of the lake beds--mainly the formation of pyrite--has largely destroyed detrital magnetite which was originally abundant in these beds. This alteration, combined with apparent CRM components, have obscured the magnetic polarity stratigraphy.

The confusing and unsatisfactory polarity zonation seems to arise at least partly from the presence of both primary and secondary remanent magnetizations. Rocks that contain detrital magnetite may have a dominant DRM, but rocks in which most or all such magnetite was destroyed may have a dominant CRM. Thermal demagnetization and studies of magnetic mineralogy suggest that the inferred CRM is carried by magnetite and (or) maghemite. We have not observed petrographically the CRM carriers, which must be present in very small amounts (<0.003 weight percent), and we do not understand how they formed. One possibility is that the CRM carriers formed via the incipient oxidation of pyrite.

One conclusion of the work to date is that the apparently reliable polarities commonly come from the stronger, coarse-grained samples, simply because these

samples tend to contain remnants of detrital magnetic minerals. Based upon our somewhat limited reliable polarity data, including the results from ash-flow tuffs and graded tuffs at the bottom of both cores, along with the strongest of the lacustrine sediments, we have found no convincing evidence for a true polarity reversal within the Creede Formation.

ACKNOWLEGMENTS

We express deep gratitude to Phil Bethke, Pete Lipman, and Wayne Campbell for their support and encouragement in many respects and to D. Larsen, D. Finkelstein, and P. Nelson for useful discussions. Doug Yager is thanked for a helpful technical review. We gratefully acknowledge the technical assistance of the drill-site science team (F. Gay, J. Hulen, D. Hayba, A. Hopkins, R. Streufert) and laboratory work by W. Rivers, J. Kahn, and P. Fitzmaurice. USGS Programs for the Development of Assessment Techniques and Deep Continental Studies supported the study.

REFERENCES

Beck, M.E., Sheriff, S.D., and Diehl, J.F., 1977, Further paleomagnetic results for the San Juan volcanic field of southern Colorado: Earth and Planetary Science Letters, v. 37, p. 124-130.

Bethke, P.M., and Lipman, P.W., 1987, Deep environment of volcanogenic epithermal mineralization: EOS, Transactions of the American Geophysical Union, v. 68, no. 13, p. 177, 187-189.

Bethke, P.M., Campbell, W.R., Hulen, J.B. and T.H. Moses, T.H., Jr., 1994, Overview of the Creede Caldera Continental Scientific Drilling Program: U.S. Geological Survey Open-File Report 94-260-A.

Campbell, W.R., 1993, Research drilling into the "fluid reservoir" of the Creede epithermal vein system, San Juan Mountain, Colorado, a preliminary report: Newsletter of the Society of Economic Geologists, April 1993, no. 13, p. 1, 3, 13-16

Canfield, D.E., and Berner, R.A., 1987, Dissolution and pyritization of magnetite in anoxic marine sediments: Geochimica et Cosmochimica Acta, v. 51, p. 645-659.

Dalrymple, G.B., and Lanphere, M.A., 1971, $^{40}Ar/^{39}Ar$ techniques of K-Ar dating: A comparison with the conventional technique: Earth and Planetary Science Letters, v. 12, p. 300-308.

Dalrymple, G.B., and Lanphere, M.A., 1974, $^{40}Ar/^{39}Ar$ age spectra of some undisturbed terrestrial samples: Geochimica et Cosmochimica Acta, v. 38, p. 715-738.

Dalrymple, G.B., Alexander, E.C., Jr., Lanphere, M.A., and Kraker, G.P., 1981, Irradiation of samples for $^{40}Ar/^{39}Ar$ dating using the Geological Survey TRIGA reactor: U.S. Geological Survey Professional Paper 1176.

Dimanche, F., and Bartholomé, P., 1976, The alteration of ilmenite in sediments: Minerals Science and Engineering, v. 8, no. 3, p. 187-201.

Harland, W.B., Armstrong, R.L., Cox, A.V., Craig, L.E., Smith A.G., and Smith, D.G., 1990, A geologic time scale 1989: Cambridge, Cambridge University Press, 263 p.

Hoblitt, R.P., and Kellogg, K.S., 1979, Emplacement temperature of unsorted and unstratified deposits of volcanic rock debris as determined by paleomagnetic techniques: Geological Society of America Bulletin, v. 90, p. 633-6442.

Hoffman, K.A., 1975, Cation diffusion and self-reversal of thermoremanent magnetization in the ilmenite-hematite solid-solution series: Geophysical Journal of the Royal Astronomical Society, v. 41, p. 65-80.

Hulen, J.B., 1992, Field geologic log summaries (1 in.=12 ft.) for coreholes CCM-2 (airport 1-6) and CCM-1 (Hosselkus 1-10): University of Utah Research Institute, DOE/ER/14207-1, ESL-92001-TR, 40 p.

Jacobs, J.A., 1984, Reversals of the Earth's magnetic field: Bristol, Adam Hilger Ltd., 230 p.

Kirschvink, J.L., 1980, The least-squares line and the analysis of palaeomagnetic data: Geophysical Journal of the Royal Astronomical Society, v. 62, p. 699-718

Lanphere, M.A., 1988, High-resolution $^{40}Ar/^{39}Ar$ chronology of Oligocene volcanic rocks, San Juan Mountains, Colorado: Geochimica et Cosmochimica Acta, v. 52, p. 1425-1434.

Lanphere, M.A., 1994, Duration of sedimentation of the Creede Formation, U.S. Geological Survey Open-File Report 94-260-C.

Larsen, D., and Crossey, L.J., 1994, Depositional environments and authigenic mineral distributions in the Oligocene Creede Formation, Colorado, USA, U.S. Geological Survey Open-File Report 94-260-E.

Larsen, D. and Nelson, P.H., 1999, Stratigraphy, Correlation, Depositional Setting, and Geophysical Characteristics of The Oligocene Snowshoe Mountain Tuff and Creede Formation In Two Cored Boreholes: Chapter 8 *in* Bethke, P.M., and Hay, R.L., eds., Geological Society of America Special Paper 346.

Lipman, P.W. and Weston, P.E., 1994, Phenocryst compositions of late ash-flow tuffs From the central San Juan caldera cluster: Results from Creede drill-hole samples and implications for regional stratigraphy: , U.S. Geological Survey Open-File Report 94-260-B.

McFadden, P.L., and Reid, A.B., 1882, Analysis of palaeomagnetic inclination data: Geophysical Journal of the Royal Astronomical Society, v. 69, p. 307-319.

Nelson, P.H., and Kibler, J.E., 1994, Geophysical logging and log processing boreholesCCM-1 and CCM-2, Creede, Colorado: U.S. Geological Survey Open-File Report 94-260-P.

Reynolds, R.L., 1982, Postdepositional alteration of titanomagnetite in a Miocene sandstone, south Texas U.S.A.: Earth and Planetary Science Letters, v. 61, p. 381-391.

Rosenbaum, J.G., Reynolds, R.L., Lipman, P.W., and Sawyer, D.A., 1987, Paleomagnetism of Oligocene ash-flow tuffs, central San Juan Mountains, Colorado: Geological Society of America Abstracts with Program, v. 19, no. 5, p. 330.

Steven, T.A., and Ratté, J.C., 1973, Geologic map of the Creede quadrangle, Mineral and Saguache Counties, Colorado: U.S. Geological Survey GQ-1053.

Steven, T.A., and Lipman, P.W., 1973, Geologic map of the Spar City quadrangle, Mineral County, Colorado: U.S. Geological Survey GQ-1052.

Tanaka, H., and Kono, M., 1973, Paleomagnetism of the San Juan volcanic field, Colorado, U.S.A.: Rock Magnetism and Paleogeophysics, v. 1, p. 71-76.

Zijderveld, J.D.A., 1967, A.C. demagnetization of rocks: Analysis of results, in Collinson, D.W, Creer, K.M., and Runcorn, S.K., eds., Methods in palaeomagnetism: Amsterdam, Elsevier, p. 254-286.

EXPLANATION: TABLES 1 AND 2

Table 1. Summary of magnetic-property data, cores CCM-1 and CCM-2.

CORE: Hole designation. CCM-1 is listed as 1, CCM-2 as 2.
RUN: Core run number.
SAMPLE: Sample depth in feet from the top of a particular core run.
SUB: Subsample A, designation given to samples that were measured for paleomagnetic direction and moment. These samples were standard paleomagnetic specimens, a cylinder 2.54 cm in diameter and about 2 cm high.
DEPTH, FT: Sample depth in feet below the drill collar.
DEPTH, M: Sample depth in meters below the drill collar.
VOLUME: Sample volume in cm^3.
MASS: Sample mass in grams.
LFMS: Low-field magnetic susceptibility. Magnetic susceptibility, in emu, measured at 600 Hz in a field of 0.1 millitesla (mT). Measurements were made using a Sapphire Instruments SI-2 susceptometer. Susceptibility in SI volume (dimensionless) units is calculated by dividing susceptibility in emu by sample volume and multiplying by 4π.
HFMS: High-field magnetic susceptibility. Magnetic susceptibility, in emu, measured at 6000 Hz in a field of 0.1 millitesla (mT). Measurements were made using a Sapphire Instruments SI-2 susceptometer. Blank entries indicate samples for which HFMS was not measured.
J: Moment (intensity of NRM) in emu. Measurements were made on several instruments, as listed in the column INSTR. Moment in SI units (Amperes/meter, A/m) is calculated by dividing moment in emu by sample volume and multiplying by 1000.
D: Magnetic declination derived from a least-squares line fitting of demagnetization decay paths. Samples were oriented vertically, but not azimuthally; declination is given as degrees clockwise from an arbitrary north. Remanent declination for these samples is not a measure of the ancient magnetic field direction. Asterisk (*) denotes sample whose demagnetization path was too erratic to confidently assign a linear fit.
I: Magnetic inclination derived from a least-squares line fitting of demagnetization decay paths, positive downward. Asterisk (*) denotes sample whose demagnetization path was too erratic to confidently assign a linear fit.
DM: Demagnetization method. A = Alternating field demagnetization, typically in 10 steps from 5 mT to 80 mT peak induction. T = Thermal demagnetization typically in 8 steps from 100°C to 600°C.
IN: Instrument used to make paleomagnetic measurements. D = 5-Hz Schonstedt DSM-1 spinner magnetometer (sensitivity of 5×10^{-7} emu/cc, or 5×10^{-4} A/m). J = 90-

Hz Geofysika JR5 spinner magnetometer (sensitivity of $1x10^{-11}$, or $1x10^{-8}$ A/m). C = cryogenic magnetometer (sensitivity of $1x10^{-11}$, or $1x10^{-8}$ A/m).
LITHOLOGY: Lithologic description of sample. Descriptions are for the paleomagnetic samples collected and in some cases may differ from the descriptions for a particular interval given in Hulen et al. (1992).

Table 2. Summary of sulfur and magnetic-susceptibility data, cores CCM-1 and CCM-2.

CORE: Hole designation. CCM-1 is listed as 1, CCM-2 as 2.
RUN: Core run number.
SAMPLE: Sample depth from the top of a particular core run.
SUB: Subsample P, designation for samples that were powdered for chemical analysis. P samples have the same depth and lithologic description as the corresponding A samples in Table 1. Subsamples designated P* were powdered sample splits provided by P. Bethke (U.S.G.S., Reston, VA) and have no corresponding paleomagnetic specimen in Table 1. Chemical analyses were determined by induction furnace (LECO) method.
S: Total sulfur, in weight percent.
LFMS: Low-field magnetic susceptibility, determined for powdered samples later submitted for chemical analysis. Magnetic susceptibility, in emu/gram, measured at 600 Hz in a field of 0.1 millitesla (mT). Measurements were made using a Sapphire Instruments SI-2 susceptometer. Susceptibility in SI mass units (m^3/kilogram) units is calculated by multiplying susceptibility in emu/gram by $4\pi \times 10^{-3}$.

Table 1. Paleomagnetic data, CCM-1 and CCM-2

CORE	RUN	SAMPLE	SUB	Depth,ft	Depth,m	Volume	Mass	LFMS	HFMS	J	D	I	DM	IN	Lithology
1	13	7.4	A	130.0	39.62	11.28	21.9	2.83E-04	2.74E-04	1.470E-04	25.7	39.4	A	D	conglomerate
1	14	0.2	A	132.8	40.48	11.83	18.3	4.45E-04	4.35E-04	2.739E-04	285.9	-27.7	A	D	conglomerate
1	14	2.5	A	135.1	41.18	11.3	21.3	1.13E-03	1.11E-03	9.315E-04	304.6	-33.5	A	D	conglomerate
1	14	7	A	139.6	42.55	11.73	26	3.91E-03	3.75E-03	3.690E-03	129.7	74.5	A	D	conglomerate; clast
1	15	1.5	A	144.1	43.92	11.02	19.9	7.58E-04	7.24E-04	3.577E-04	295.6	-26.5	A	D	conglomerate
1	15	8.3	A	150.9	45.99	11.24	24.8	1.66E-03	1.63E-03	1.355E-03	295.2	19.7	A	D	conglomerate
1	16	3.7	A	156.3	47.64	10.75	19.5	8.56E-04	8.37E-04	3.992E-04	145.1	21.3	A	D	conglomerate
1	16	7.5	A	160.1	48.80	11.39	16.6	6.48E-04	6.44E-04	1.101E-03	204.2	54.5	A	D	coarse-grained sandstone
1	17	2.45	A	165.1	50.31	10.49	16.4	4.10E-04	4.05E-04	2.241E-04	37.4	5.7	A	D	coarse-grained sandstone
1	17	6.2	A	168.8	51.45	11.35	20.7	6.78E-04	6.59E-04	2.816E-04	36.1	39.5	A	D	conglomerate
1	18	9.4	A	182.0	55.47	11.43	23.7	7.51E-04	7.56E-04	2.308E-03	32.2	-74	A	D	conglomerate; clast
1	19	0.6	A	183.2	55.84	11.13	22.2	1.24E-03		1.860E-03	180.3	-69.3	T	D	conglomerate
1	19	1.9	A	184.5	56.24	11.34	22.5	3.55E-04	3.48E-04	4.464E-04	352.1	60	A	D	conglomerate
1	19	2.9	A	185.5	56.54	11.58	20	7.33E-05	7.86E-05	1.859E-05	*	*	A	D	sandstone
1	23	6.3	A	228.9	69.77	11.1	18.8	1.33E-04	1.30E-04	1.766E-05	278.4	-30.5	T	J	sandstone
1	23	6.45	A	229.1	69.81	1.56	19.26	1.27E-04	1.27E-04	4.993E-06	315.6	-25.8	A	J	fine-grained sandstone
1	25	3.15	A	243.7	74.26	10.85	19.94	6.82E-05	7.16E-05	8.548E-06	359	34.2	A	J	fine-grained sandstone
1	25	3.3	A	243.8	74.31	11	21.79	7.60E-05	7.87E-05	4.629E-06	*	*	T	J	fine-grained sandstone
1	25	5.15	A	245.7	74.87	10.8	22.22	4.57E-05	4.94E-05	4.312E-06	*	*	T	J	fine-grained sandstone
1	25	5.3	A	245.8	74.92	10.94	23.15	4.93E-05	5.28E-05	7.480E-06	154.9	-41.1	A	J	fine-grained sandstone
1	27	1	A	251.0	76.50	10.95	21.44	7.22E-05	7.45E-05	1.977E-05	15.3	47	T	J	fine-grained sandstone
1	27	1.2	A	251.2	76.57	10.7	20.7	6.51E-05	6.72E-05	1.397E-05	359.9	50	A	J	fine-grained sandstone
1	27	2.05	A	252.1	76.82	10.9	21.65	9.75E-05	9.79E-05	3.807E-05	56.3	75.6	T	J	fine-grained sandstone
1	27	2.15	A	252.2	76.86	11.73	24.9	1.54E-04	1.54E-04	3.490E-05	283	-46.6	A	D	coarse-grained sandstone
1	27	3.7	A	253.7	77.33	10.98	23.69	3.37E-04	3.29E-04	1.380E-04	46.7	45.7	T	J	coarse-grained sandstone
1	27	3.8	A	253.8	77.36	11.28	24.9	4.72E-04	4.61E-04	1.679E-04	268.8	53.1	A	D	coarse-grained sandstone
1	27	8.4	A	258.4	78.76	10.84	20.52	3.34E-04	3.25E-04	1.379E-04	*	*	A	J	coarse-grained sandstone
1	27	8.5	A	258.5	78.79	11.4	21.4	7.34E-04		8.160E-04	108	18	T	D	coarse-grained sandstone
1	28	2.8	A	263.2	80.22	10.77	19.15	4.10E-04	4.00E-04	8.570E-05	*	*	T	J	coarse-grained sandstone
1	28	4.4	A	264.8	80.71	11.29	21.6	7.13E-04	7.08E-04	3.925E-04	88.1	63.6	A	D	conglomerate
1	28	4.5	A	264.9	80.74	10.94	21.06	8.73E-04	8.62E-04	1.560E-04	13.9	-45.5	T	J	conglomerate
1	28	9.3	A	269.7	82.20	10.75	20.95	9.52E-04	9.27E-04	8.111E-04	329.9	-4.6	A	J	conglomerate
1	28	9.4	A	269.8	82.24	11.58	21.4	8.01E-04		3.130E-04	142.4	36.4	T	D	conglomerate
1	29	6.7	A	277.0	84.43	10.37	17.13	3.78E-04	3.64E-04	2.316E-04	157.6	8.9	T	J	coarse-grained sandstone
1	29	6.8	A	277.1	84.46	11.21	20.6	4.14E-04	4.02E-04	2.209E-04	257.8	64.6	A	D	coarse-grained sandstone
1	30	3.1	A	283.6	86.44	11.14	23.3	6.42E-04	6.33E-04	3.702E-04	124.3	40.3	A	D	conglomerate
1	30	3.2	A	283.7	86.47	10.95	20.21	6.16E-04	6.03E-04	3.252E-04	138	46.6	T	J	conglomerate
1	30	4.8	A	285.3	86.96	10.77	18.74	1.27E-04	1.24E-04	1.961E-05	*	*	T	J	fine-grained sandstone
1	30	4.9	A	285.4	86.99	11.44	19.3	1.78E-04	1.75E-04	4.199E-05	*	*	A	D	fine-grained sandstone
1	31	3.5	A	291.0	88.70	11.04	23.73	9.56E-05	9.64E-05	4.838E-05	37	60.4	A	J	siltstone
1	31	3.6	A	291.1	88.73	10.98	21.1	8.55E-05	8.62E-05	2.360E-06	*	*	T	D	siltstone
1	31	8.3	A	295.8	90.16	10.98	19.22	9.66E-05	9.72E-05	1.515E-05	318.2	41.4	T	J	siltstone
1	31	8.4	A	295.9	90.19	10.8	18.48	1.05E-04	1.03E-04	1.659E-05	311.8	-45.4	A	J	siltstone

Table 1. Paleomagnetic data, CCM-1 and CCM-2

CORE	RUN	SAMPLE	SUB	Depth,ft	Depth,m	Volume	Mass	LFMS	HFMS	J	D	I	DM	IN	Lithology
1	34	0.7	A	312.9	95.37	11.08	22.87	6.07E-05	6.31E-05	1.476E-05	303.8	-58.6	A	J	sandstone
1	34	0.9	A	313.1	95.43	11.03	22	6.68E-05	6.94E-05	1.804E-05	151.6	27.1	T	J	sandstone
1	34	7.1	A	319.3	97.32	11.38	24.05	5.89E-05	6.12E-05	2.093E-05	35.5	57.3	A	J	sandstone
1	34	7.2	A	319.4	97.35	10.72	22.01	6.92E-05	7.38E-05	3.762E-05	154.5	30.1	T	J	sandstone
1	34	8.6	A	320.8	97.78	10.7	19.74	7.19E-05	7.39E-05	2.529E-05	62.7	61.6	A	J	siltstone
1	34	8.7	A	320.9	97.81	10.65	18.86	7.53E-05	7.69E-05	2.549E-05	146.9	15.9	T	J	siltstone
1	36	3.9	A	336.2	102.47	11.63	20.1	5.23E-05	5.88E-05	6.110E-06				C	reworked tuff
1	36	5.1	A	337.4	102.84	11.48	19.9	4.39E-05	4.86E-05	8.282E-06	356.3	51.8	A	D	reworked tuff
1	45	3.65	A	406.2	123.79	10.85	24.8	7.53E-04		4.330E-03	332.1	76.8	T	D	sandstone
1	45	5.5	A	408.0	124.36	11.24	21.2	2.48E-04		5.680E-05	227.1	-42.9	A	C	sandstone
1	52	2.1	A	473.6	144.35	11.73	21.2	6.61E-05	7.39E-05	1.153E-05	0.8	58	A	D	reworked tuff
1	52	9.2	A	480.7	146.52	11.33	19.8	5.15E-05	5.66E-05	1.185E-05	112.1	39.2	A	D	reworked tuff
1	53	6.2	A	486.9	148.41	11.53	21.4	9.56E-05	9.95E-05	3.520E-05				C	reworked tuff
1	55	2.9	A	492.6	150.14	11.29	22.1	4.12E-04		5.590E-05	181	-41.5	T	D	fine-grained sandstone
1	56	2.8	A	497.5	151.64	11.1	21.7	5.88E-04	5.59E-04	1.719E-04	269.9	54.5	A	D	fine-grained sandstone
1	57	0.8	A	501.5	152.86	11.04	21.5	7.91E-04	7.55E-04	1.550E-04				C	sandstone
1	57	1.7	A	502.4	153.13	11.01	21.9	7.55E-04	7.18E-04	1.119E-04	194	62.8	A	D	sandstone
1	60	6.4	A	536.5	163.53	11.13	20.86	7.09E-05	7.17E-05	2.129E-05	*	*	A	J	fine-grained sandstone
1	60	6.5	A	536.6	163.56	10.95	21.41	8.74E-05	8.68E-05	2.367E-05	175	1.4	T	J	fine-grained sandstone
1	62	0.7	A	550.9	167.91	11.04	20.88	7.30E-05	7.68E-05	1.506E-05	41.1	67.8	A	J	fine-grained sandstone
1	62	0.8	A	551.0	167.95	10.47	20.06	1.06E-04	1.09E-04	1.497E-05	163.6	0.6	T	J	fine-grained sandstone
1	63	1.5	A	561.9	171.27	11.24	23.61	2.28E-04	2.21E-04	6.984E-05	356.9	62.7	A	J	fine-grained sandstone
1	63	1.6	A	562.0	171.30	10.8	22.07	1.31E-04	1.29E-04	4.444E-05	163	25.5	T	J	fine-grained sandstone
1	63	2.8	A	563.2	171.66	10.46	20.66	9.43E-05	9.25E-05	2.306E-05	*	*	A	J	fine-grained sandstone
1	63	2.9	A	563.3	171.69	10.8	21.14	1.18E-04	1.17E-04	3.164E-05	350.4	39.3	T	J	fine-grained sandstone
1	65	4.7	A	576.1	175.60	10.9	22.17	1.45E-04	1.41E-04	4.776E-05	61.8	39.7	T	J	fine-grained sandstone
1	65	4.9	A	576.3	175.66	10.85	21.56	1.15E-04	1.13E-04	2.277E-05	71.4	-81.9	A	J	fine-grained sandstone
1	66	2.05	A	580.0	176.77	10.65	19.53	7.99E-05	8.19E-05	7.507E-06	148.4	-24.7	A	J	reworked tuff
1	66	2.2	A	580.1	176.81	10.65	19.54	8.04E-05	8.25E-05	1.327E-05	*	*	T	J	reworked tuff
1	66	3.2	A	581.1	177.12	10.8	19.4	8.70E-05	9.01E-05	9.957E-06	*	*	T	J	reworked tuff
1	66	3.3	A	582.2	177.45	11.44	20.5	9.32E-05	9.70E-05	7.284E-06	151.3	-24.7	A	J	reworked tuff
1	67	1.7	A	587.1	178.95	11.48	21.3	8.64E-05	8.96E-05	1.264E-05	96.1	73.8	A	J	reworked tuff
1	67	1.8	A	587.2	178.98	10.9	20.08	8.05E-05	8.51E-05	1.471E-05	166.4	-1.6	T	J	reworked tuff
1	67	5.55	A	591.0	180.12	10.84	25.08	2.08E-04	2.03E-04	8.738E-05	*	*	A	J	sandy reworked tuff
1	67	5.65	A	591.1	180.15	10.9	22.36	1.93E-04	1.88E-04	7.456E-05	134.1	-4.9	T	J	sandy reworked tuff
1	67	7.2	A	592.6	180.62	10.89	21.85	2.09E-04	2.07E-04	9.740E-05	125.7	16.1	A	J	coarse-grained sandstone
1	67	7.3	A	592.7	180.66	10.69	21.88	2.85E-04	2.81E-04	1.141E-04	124.8	4.1	T	J	coarse-grained sandstone
1	68	0.6	A	596.3	181.75	10.94	20.97	1.21E-04	1.21E-04	3.387E-05	351.6	66.9	A	J	fine-grained sandstone
1	68	0.7	A	596.4	181.78	10.95	21.61	1.16E-04	1.15E-04	2.343E-05	66.7	-17.1	T	J	fine-grained sandstone
1	69	0.5	A	601.7	183.40	10.84	22	9.03E-05	8.91E-05	1.305E-05	*	*	T	J	reworked tuff
1	69	0.6	A	601.8	183.43	11.13	22.41	9.62E-05	9.56E-05	9.856E-06	269.9	-32.6	A	J	reworked tuff
1	70	2	A	613.5	187.00	10.7	19.75	5.61E-05	5.98E-05	3.161E-06	10.8	62	T	J	reworked tuff
1	70	2.1	A	613.6	187.03	11.24	20.8	5.77E-05	6.31E-05	4.591E-06	95.2	9.3	A	J	reworked tuff

Table 1. Paleomagnetic data, CCM-1 and CCM-2

CORE	RUN	SAMPLE	SUB	Depth,ft	Depth,m	Volume	Mass	LFMS	HFMS	J	D	I	DM	IN	Lithology
1	70	8.5	A	620.0	188.98	100.58	18.69	6.84E-05	7.20E-05	2.827E-05	*	*	A	J	reworked tuff
1	70	8.6	A	620.1	189.01	11.33	20	7.12E-05	7.68E-05	4.648E-06	112.2	-3.6	T	J	reworked tuff
1	71	1.5	A	622.9	189.86	10.85	19.02	7.65E-05	8.01E-05	1.032E-05	152.4	8.7	T	J	reworked tuff
1	71	1.6	A	623.0	189.89	11	19.6	7.83E-05	8.22E-05	7.979E-06	86.9	61.6	A	J	reworked tuff
1	73	5.15	A	646.7	197.10	11.24	21	9.30E-05	9.46E-05	1.599E-05	*	*	A	D	reworked tuff
1	73	8.8	A	650.3	198.21	11.53	21.1	9.06E-05		1.770E-05	190.3	-44.9	T	D	fine-grained sandstone
1	74	1.5	A	653.1	199.07	11.19	21	1.20E-04	1.22E-04	9.375E-06	223.1	-49	A	D	sandstone
1	74	2.85	A	654.5	199.48	11.1	27.4	3.12E-02	3.10E-02	1.027E-02	3	30.5	A	D	coarse-grained sandstone
1	74	3.15	A	654.8	199.57	10.87	25.7	7.80E-03		2.370E-03	349.2	60.1	T	D	reworked tuff
1	74	3.5	A	655.1	199.67	11.27	21.1	1.59E-04	1.58E-04	1.998E-05	191.1	-29.5	A	D	coarse-grained sandstone
1	75	10.4	A	671.9	204.80	11.39	21	1.00E-04		4.975E-06	7.9	-38.3	A	C	reworked tuff
1	76	2.8	A	674.5	205.59	11.14	25.1	9.84E-05	1.02E-04	1.580E-05	324	51.6	A	C	reworked tuff
1	84	5.5	A	743.7	226.68	10.85	18.2	4.31E-05	4.74E-05	1.375E-06	323.5	-24.6	A	C	reworked tuff
1	84	9.6	A	747.8	227.93	11.54	24.1	5.89E-05	6.56E-05	1.495E-06	330.5	-36.6	A	C	reworked tuff
1	97	9.3	A	871.1	265.51	11.28	28.9	9.40E-04	9.10E-04	7.444E-04	67.5	44.4	A	D	sandstone
1	100	5.2	A	897.0	273.41	11.43	24.1	9.79E-05		9.907E-05	282.8	-31.9	A	C	sandy reworked tuff
1	102	9.25	A	921.0	280.71	11.08	23.7	1.87E-04		4.708E-05	*	*	A	C	sandy reworked tuff
1	105	7.9	A	939.7	286.42	11.28	24.7	9.19E-05		3.121E-05	194.9	23.5	A	D,C	sandy reworked tuff
1	107	6.3	A	958.1	292.03	11.53	26.3	8.22E-05		5.635E-05	103.5	29.3	A	D,C	sandy reworked tuff
1	109	2.4	A	974.2	296.94	11.43	24.2	1.38E-04		4.164E-05	99.2	23.5	A	D,C	sandy reworked tuff
1	110	1.7	A	984.0	299.92	11.53	24.7	4.27E-04	4.21E-04	2.178E-04	85.5	-22.2	A	D,C	coarse-grained sandstone
1	111	2.9	A	994.0	302.97	11.33	24.2	4.83E-04		1.555E-04	44.9	-27.4	A	D,C	conglomerate
1	112	1.35	A	998.0	304.18	11.88	28.5	3.71E-04	3.52E-04	1.808E-03	181.3	-27.8	A	D	conglomerate
1	113	3.4	A	1004.9	306.29	11.33	24.5	1.33E-03	1.31E-03	8.768E-04	*	*	A	D	conglomerate
1	114	5.65	A	1017.8	310.21	11.28	27.9	2.06E-01		1.600E-01	71.3	80.9	A	D	conglomerate
1	115	4.6	A	1026.7	312.94	11.33	24.7	8.59E-03		2.266E-03	4.9	54.7	A	D	sandstone
1	117	0.65	A	1041.5	317.43	11.63	25.6	6.26E-03	6.19E-03	1.205E-03	341.6	80.6	A	D	sandy reworked tuff
1	118	5.6	A	1054.7	321.47	10.95	20.7	9.80E-03	9.76E-03	5.700E-04	354.8	-51.9	A	D	coarse-grained sandstone
1	118	5.85	A	1055.0	321.55	11.38	22.3	9.55E-02		4.734E-02	339.1	18.8	A	D	coarse-grained sandstone
1	120	6.55	A	1068.0	325.51	11.43	24.5	2.77E-02	2.74E-02	6.929E-03	319.9	78.5	A	D	conglomerate
1	120	6.9	A	1068.3	325.62	12.02	28.9	4.18E-03	4.17E-03	4.955E-03	295.5	2.2	A	D,C	conglomerate; clast
1	121	7.6	A	1079.1	328.91	11.53	27.7	2.37E-01		1.863E-01	31.1	67.3	A	D	conglomerate
1	122	3.3	A	1084.5	330.56	11.38	24.2	2.54E-02		1.615E-02	359.6	-5.9	A	D	conglomerate
1	122	3.45	A	1084.7	330.60	11.78	30	1.17E-02		1.679E-02	171.3	11.6	A	D	conglomerate
1	124	8.15	A	1102.7	336.09	11.53	26	2.28E-02	2.26E-02	1.500E-02	14.1	71.4	A	D	conglomerate
1	124	8.35	A	1102.9	336.15	11.48	29.5	1.11E-02	1.10E-02	4.334E-02	146.7	22.8	A	D	conglomerate; clast
1	126	1.35	A	1113.0	339.23	11.54	22	2.01E-02		9.740E-03	12.8	72.9	T	D	coarse-grained sandstone
1	126	1.55	A	1113.2	339.29	11.09	28.1	8.04E-03		9.610E-03	75	-37.1	T	D	conglomerate; clast
1	127	6.2	A	1127.7	343.72	11.63	24.2	2.30E-04	2.30E-04	1.910E-04	127.9	44.5	A	D	fine-grained reworked tuff
1	128	1.7	A	1132.0	345.03	11.03	20.7	8.72E-04	8.63E-04	2.930E-04	*	*	A	D	reworked tuff
1	128	5.6	A	1135.9	346.22	11.43	23.3	5.39E-03	5.34E-03	1.675E-03	*	*	A	D	reworked tuff
1	128	10.2	A	1140.5	347.63	11.38	21.7	1.88E-02	1.85E-02	1.154E-02	122.8	76.2	A	D	coarse-grained reworked tuff
1	129	5.5	A	1146.1	349.33	11.58	23.7	1.23E-02	1.22E-02	5.320E-03				C	coarse-grained reworked tuff

Table 1. Paleomagnetic data, CCM-1 and CCM-2

CORE	RUN	SAMPLE	SUB	Depth,ft	Depth,m	Volume	Mass	LFMS	HFMS	J	D	I	DM	IN	Lithology
1	129	7.15	A	1147.8	349.83	11.18	22.8	9.19E-03	9.11E-03	6.290E-03				C	coarse-grained reworked tuff
1	129	7.9	A	1148.5	350.06	11.18	24.1	6.14E-03	6.09E-03	1.420E-03				C	coarse-grained reworked tuff
1	130	1.3	A	1150.2	350.58	11.08	22	1.15E-03	1.14E-03	1.043E-03	19.1	40.2	A	D	reworked tuff
1	130	8.4	A	1157.3	352.75	11.08	21.9	1.56E-04	1.57E-04	1.453E-04	248	53.1	A	D	reworked tuff
1	131	2.7	A	1160.4	353.69	11.34	21.4	3.17E-04	3.18E-04	2.218E-04	245.8	66.9	A	D	reworked tuff
1	131	3.6	A	1161.3	353.96	11.38	20.6	1.54E-03	1.53E-03	5.768E-04	239.8	73.5	A	D	reworked tuff
1	131	5.1	A	1162.8	354.42	11.2	20.3	2.09E-03	2.07E-03	9.913E-04	281.6	58.3	A	D	reworked tuff
1	131	7.5	A	1165.2	355.15	11.05	20.3	3.48E-03	3.44E-03	6.180E-04	168.8	64.6	A	D,C	reworked tuff
1	131	9.6	A	1167.3	355.79	11.48	22.7	4.14E-03	4.11E-03	1.019E-03	224.9	60.4	A	D	reworked tuff
1	132	3.4	A	1171.6	357.10	11.19	20.6	6.20E-03	6.15E-03	3.336E-03	2.7	68.6	A	D	reworked tuff
1	132	9.2	A	1177.4	358.87	11.63	21.4	9.68E-03	9.62E-03	6.900E-03				C	reworked tuff
1	133	7.4	A	1185.9	361.46	11.53	21.9	1.50E-02	1.49E-02	3.874E-03	14	70.5	A	D	reworked tuff
1	134	2.2	A	1191.0	363.02	11.23	21.3	1.61E-02	1.60E-02	4.677E-03	2.2	71.6	A	D	reworked tuff
1	134	8.2	A	1197.0	364.85	11.43	21.7	1.82E-02	1.80E-02	2.874E-03	5.9	75.2	A	D	reworked tuff
1	135	1.1	A	1200.0	365.76	11.18	22.2	2.19E-02	2.17E-02	6.003E-03	142.6	87.6	A	D	reworked tuff
1	135	2.7	A	1201.6	366.25	11.58	23.3	2.80E-02	2.78E-02	1.069E-02	325.6	85.9	A	D	reworked tuff
1	135	3.3	A	1202.2	366.43	11.53	22.7	2.03E-02	2.01E-02	7.770E-03				C	coarse-grained sandstone
1	135	4.7	A	1203.6	366.86	11.68	23.6	2.53E-02	2.51E-02	6.780E-03				C	coarse-grained sandstone
1	135	6.4	A	1205.3	367.38	11.73	27.8	2.87E-03	2.87E-03	1.800E-03				C	tuff breccia
1	136	3.2	A	1212.4	369.54	11.68	27.1	4.36E-03	4.34E-03	1.580E-03				C	tuff breccia
1	136	8.5	A	1217.7	371.16	12.02	29.4	2.38E-03	2.39E-03	1.430E-03				C	tuff breccia
1	137	1.3	A	1220.5	372.01	11.48	27.7	8.74E-04	8.74E-04	3.580E-03				C	tuff breccia
1	137	6.2	A	1225.4	373.50	11.63	26.5	2.55E-04	2.61E-04	1.330E-03				C	tuff breccia
1	138	2.7	A	1232.0	375.51	11.73	27.9	4.13E-03	4.11E-03	2.810E-03				C	tuff breccia
1	138	8.2	A	1237.5	377.19	11.38	25.9	2.32E-04	2.36E-04	1.840E-03				C	tuff breccia
1	139	1.1	A	1240.7	378.17	11.48	26.2	1.43E-04	1.50E-04	3.850E-03				C	tuff breccia
1	139	2.5	A	1242.1	378.59	11.97	25.7	2.65E-04	2.53E-04	3.100E-03				C	tuff breccia
1	139	4.2	A	1243.8	379.11	11.53	24.2	1.99E-04	1.80E-04	9.160E-04				C	tuff breccia
1	140	1.25	A	1251.3	381.38	11.48	26.2	9.27E-03	9.20E-03	2.850E-03				C	tuff breccia
1	140	9.8	A	1259.8	383.99	11.97	26.3	8.60E-03	8.51E-03	4.970E-03	*	*	A	D,C	tuff breccia
1	141	4.4	A	1264.7	385.48	11.92	28.5	5.41E-03	5.38E-03	4.720E-03				C	tuff breccia
1	142	3.7	A	1274.2	388.38	11.48	22.4	1.47E-02	1.46E-02	6.230E-03	357.3	51.5	A	D,C	tuff breccia
1	143	0.4	A	1281.2	390.51	11.33	23.7	1.62E-02	1.61E-02	9.190E-03				C	tuff breccia
1	143	7.5	A	1288.3	392.67	11.58	23.6	1.47E-02	1.45E-02	1.090E-02	157.2	67.9	A	D,C	tuff breccia
1	144	6.5	A	1297.1	395.36	12.27	29.2	5.86E-03	5.83E-03	3.750E-03				C	tuff breccia
1	145	3.9	A	1304.7	397.67	11.38	23.7	9.17E-03	9.09E-03	4.060E-03	289	10.2	A	D,C	tuff breccia
1	145	5.3	A	1306.1	398.10	11.88	15.7	1.15E-03	1.15E-03	1.327E-03	270.9	-33.7	A	D	tuff breccia
1	145	6.8	A	1307.6	398.56	11.19	16.8	1.15E-03	1.14E-03	1.440E-03	276.9	-28.2	A	D,C	tuff breccia
1	146	5.5	A	1316.7	401.33	11.39	23.2	1.46E-02	1.45E-02	3.790E-03				C	tuff breccia
1	147	4.5	A	1325.7	404.07	11.49	23.4	1.36E-02	1.34E-02	7.370E-03				C	tuff breccia
1	148	5.3	A	1336.3	407.31	11.12	23.5	1.03E-02	9.77E-03						tuff breccia
1	149	2.3	A	1343.6	409.53	12.02	27	2.56E-02	2.55E-02	2.020E-02	141	71.3	A	D,C	tuff breccia
1	150	1.3	A	1353.1	412.43	11.48	23.3	1.47E-02	1.45E-02						tuff breccia

Table 1. Paleomagnetic data, CCM-1 and CCM-2

CORE	RUN	SAMPLE	SUB	Depth,ft	Depth,m	Volume	Mass	LFMS	HFMS	J	D	I	DM	IN	Lithology
1	151	1.75	A	1363.8	415.67	11.48	27.9	5.63E-03	5.59E-03	9.110E-03				C	tuff breccia
1	151	9.4	A	1371.4	418.00	11.68	24.6	1.26E-02	1.21E-02	2.260E-02	286	16.7	A	D,C	tuff breccia
2	2	6.3	A	145.7	44.41	11.63	19.8	2.43E-04	2.39E-04	1.01E-04				C	fine-grained sandstone
2	2	8.1	A	147.5	44.96	11.19	19.5	2.85E-04	2.78E-04	1.58E-04				C	fine-grained sandstone
2	3	0.4	A	149.8	45.66	9.66	16.46	3.87E-04	3.75E-04	2.02E-04	38.4	70.3	A	D	medium-grained sandstone
2	3	0.8	A	150.2	45.78	10.97	18.11	2.87E-04	2.76E-04	1.44E-04	37	38.9	T	D	fine-grained sandstone
2	4	8.1	A	164.5	50.14	10.52	18.52	2.83E-04	2.68E-04	8.46E-05	327.7	-47.5	A	D	medium-grained sandstone
2	9	8.1	A	209.8	63.95	11.39	17.6	6.35E-05	6.77E-05	4.12E-05				C	sandy reworked tuff
2	9	9.3	A	211.0	64.31	11.58	18.1	6.33E-05	6.80E-05	1.10E-05				C	sandy reworked tuff
2	10	3.15	A	215.1	65.55	11.44	17.5	6.35E-05	6.87E-05	1.37E-05				C	reworked tuff
2	10	6.2	A	218.1	66.48	11.63	16.6	4.37E-05	4.99E-05	7.92E-06				C	reworked tuff
2	11	0.2	A	221.9	67.64	11.88	17.8	5.33E-05	6.09E-05	9.54E-06				C	airfall tuff
2	12	0.1	A	232.2	70.77	9.98	16.87	1.65E-04	1.61E-04	6.35E-05	304.6	48.2	T	D	silty reworked tuff
2	12	0.5	A	232.6	70.90	10.67	24.79	3.93E-04	3.86E-04	6.91E-05	330.8	38.1	A	D	sandy reworked tuff
2	12	0.8	A	232.9	70.99	10.67	24.08	3.23E-04	3.14E-04	1.24E-04	83.6	-57.8	A	D	sandy reworked tuff
2	12	1.2	A	233.3	71.11	10.72	26.19	5.19E-04	5.04E-04	1.42E-04	17.3	32.7	T	D	sandy reworked tuff
2	13	5.5	A	247.4	75.41	10.97	18.2	1.50E-04	1.48E-04	1.03E-04	0.8	61.1	A	D	fine-grained sandstone
2	13	10.3	A	252.2	76.87	12.08	18.7	1.67E-04	1.62E-04	6.45E-04				C	fine-grained sandstone
2	20	4.7	A	306.8	93.51	12.17	19.9	1.24E-04	1.28E-04	1.99E-05	232.3	57	A	D	sandy reworked tuff
2	20	6.9	A	309.0	94.18	11.44	20.4	1.65E-04	1.67E-04	5.13E-05				C	sandy reworked tuff
2	21	0.9	A	312.8	95.34	11.58	19	1.73E-04	1.71E-04	1.74E-05	164.2	-62.3	A	D	fine-grained sandstone; brecci
2	21	2.55	A	314.5	95.84	11.31	19.3	2.22E-04	2.12E-04	1.06E-04	349.3	49.3	A	D	sandstone; breccia matrix
2	21	6.2	A	318.1	96.96	11.98	18.8	3.51E-04	3.31E-04	1.47E-03				C	sandstone; breccia matrix
2	21	9.2	A	321.1	97.87	8.69	17.4	3.47E-04	3.28E-04	2.96E-04				C	coarse-grained sandstone; br
2	22	4.5	A	326.6	99.55	11.54	14	3.13E-04	2.93E-04	3.32E-05	163.1	-42.8	A	D	coarse-grained sandstone; br
2	22	6.2	A	328.3	100.07	10.07	19.81	4.25E-04	3.93E-04	2.09E-04	115.4	72.6	T	D	coarse-grained sandstone
2	31	2.4	A	404.3	123.23	10.9	19.4	1.63E-04	1.62E-04	3.70E-05	225.7	-52.1	A	D	sandy reworked tuff
2	31	4.2	A	406.1	123.78	11.63	18.2	1.74E-04	1.71E-04	2.91E-05				C	fine-grained sandstone
2	31	8.1	A	410.0	124.97	11.13	21.6	5.27E-04	5.10E-04	2.08E-04	101.6	45	A	D	coarse-grained sandstone
2	31	4.35	A	411.3	125.35	11.78	20.4	5.97E-04	5.76E-04	4.19E-04				C	coarse-grained sandstone
2	32	4.2	A	416.3	126.89	11.02	20.8	1.69E-04	1.69E-04	6.82E-05	312.3	-55.8	A	D	sandy reworked tuff
2	32	5.3	A	417.4	127.22	11.48	17.9	2.41E-04	2.37E-04	7.93E-05	173	59.5	A	D	sandstone
2	32	6.5	A	418.6	127.59	11.68	21.4	4.35E-04	4.14E-04	3.49E-04				C	sandstone
2	47	1.1	A	533.0	162.46	9.92	17.04	3.57E-04	3.28E-04	1.27E-04	17.7	18.8	A	D	sandstone
2	47	1.2	A	533.1	162.49	9.9	16.29	3.32E-04	3.06E-04	1.03E-04	*	*	T	D	sandstone
2	51	7	A	578.7	176.39	9.9	15.18	1.50E-04	1.45E-04	6.58E-05	246.5	-62.8	A	D	fine-grained airfall tuff
2	51	7.3	A	579.0	176.48	10.29	18.62	2.51E-04	2.39E-04	3.20E-05	194.5	-39.5	T	D	medium-grained airfall tuff
2	54	9.3	A	611.2	186.29	11.23	17.2	3.31E-05	4.06E-05	1.05E-05				C	airfall tuff
2	55	7.4	A	619.6	188.85	11.63	16.5	3.04E-05	3.57E-05	4.75E-06				C	airfall tuff
2	56	1.3	A	623.2	189.95	11.08	17	3.09E-05	3.69E-05	1.56E-05				C	airfall tuff
2	57	1.6	A	631.6	192.51	11.13	16.3	2.33E-05	2.85E-05	8.47E-06				C	airfall tuff
2	61	9	A	674.3	205.53	11.18	24.44	2.63E-04	2.54E-04	4.97E-05	332	-61.1	A	D	sandstone
2	61	9.2	A	674.5	205.59	10.82	25.94	3.31E-04	3.18E-04	1.19E-04	3.9	-19.1	T	D	sandstone

Table 1. Paleomagnetic data, CCM-1 and CCM-2

CORE	RUN	SAMPLE	SUB	Depth,ft	Depth,m	Volume	Mass	LFMS	HFMS	J	D	I	DM	IN	Lithology
2	62	2.05	A	677.3	206.43	11.18	23.7	1.23E-04	1.20E-04	3.07E-05				C	fine-grained sandstone
2	65	0.1	A	705.7	215.10	10.97	19.17	3.24E-04	3.07E-04	5.08E-05	331	-36.9	A	D	reworked tuff
2	65	0.3	A	705.9	215.16	11.71	19.77	3.22E-04	3.05E-04	7.23E-05	346.1	-11.3	T	D	sandy reworked tuff
2	76	1.2	A	811.7	247.41	10.67	16.28	9.21E-05	9.19E-05	1.30E-05	149.4	-40.7	A	D	fine-grained reworked tuff
2	76	2.6	A	813.1	247.83	10.74	16.91	3.01E-04	2.96E-04	8.43E-05	14.4	27.4	T	D	fine-grained reworked tuff
2	76	3.5	A	814.0	248.11	10.92	17.85	1.17E-03	1.15E-03	2.57E-04	13.6	6	A	D	sandy reworked tuff
2	76	3.7	A	814.2	248.17	10.87	18.13	1.28E-03	1.26E-03	4.38E-04	15.1	0.5	T	D	sandy reworked tuff
2	78	7.3	A	833.5	254.05	10.94	18.25	1.19E-04	1.18E-04	2.74E-05	*	*	A	D	fine-grained reworked tuff
2	78	8.1	A	834.3	254.30	9.13	15.81	2.78E-04	2.68E-04	7.11E-05	338.9	-9.5	T	D	fine-grained reworked tuff
2	78	8.8	A	835.0	254.51	10.42	18.39	3.53E-04	3.34E-04	9.07E-05	256.3	-54.9	A	D	sandy reworked tuff
2	78	9.3	A	835.5	254.66	8.21	15.29	2.47E-04	2.36E-04	9.71E-05	280.9	-34.3	T	D	sandy reworked tuff
2	85	3.1	A	897.5	273.56	10.27	17.8	2.14E-04	2.07E-04	1.08E-04	325.1	37.1	A	D	fine-grained sandstone
2	85	4	A	898.4	273.83	10.23	19.22	2.64E-04	2.52E-04	1.57E-04	348.6	5.8	T	D	fine-grained sandstone
2	85	4.7	A	899.1	274.05	9.8	17.28	3.11E-04	2.93E-04	9.06E-05	187.4	72.4	A	D	sandy reworked tuff
2	85	5.3	A	899.7	274.23	9.85	17.6	4.66E-04	4.34E-04	4.25E-04	32.7	7.3	A	D	sandstone
2	85	5.4	A	899.8	274.26	10.94	19.95	6.00E-04	5.55E-04	4.09E-04	41.9	-0.2	T	D	sandstone
2	86	9.2	A	913.9	278.56	10.86	19.08	4.14E-04	3.86E-04	2.51E-04	9.5	-2	T	D	sandstone
2	86	9.3	A	914.0	278.59	11.48	20.94	4.26E-04	3.96E-04	1.50E-04	2.2	70.8	A	D	sandy reworked tuff
2	93	1.2	A	970.8	295.90	11.43	18.8	4.67E-04	4.35E-04	9.76E-05				C	conglomerate; matrix
2	93	7.2	A	976.8	297.73	11.33	21.6	1.41E-03	1.31E-03	3.56E-04				C	conglomerate; matrix
2	94	5.3	A	984.8	300.17	11.18	21.4	1.52E-03	1.45E-03	5.06E-04				C	conglomerate; matrix
2	95	3.3	A	992.3	302.45	11.53	17.1	7.02E-05	7.29E-05	2.49E-05				C	reworked tuff
2	96	2.5	A	1001.2	305.17	11.73	17.4	8.87E-05	8.98E-05	4.44E-05				C	reworked tuff
2	96	7.2	A	1005.9	306.60	11.44	18.3	1.24E-04	1.31E-04	4.18E-05	54.9	65.5	A	D	reworked tuff
2	97	2.3	A	1011.1	308.18	11	18.3			6.04E-05	184.7	68.9	T	D	airfall tuff
2	97	9.4	A	1018.2	310.35	11.28	21.8	9.54E-04	8.74E-04	1.12E-04	188.6	60.8	A	D	breccia; matrix
2	98	3.4	A	1022.1	311.54	11.38	22			4.26E-04	22.9	60.2	T	D	breccia; matrix
2	98	7.4	A	1026.1	312.76	11.3	22.7	1.54E-02	1.49E-02	1.44E-03	*	*	A	D	breccia; matrix
2	99	0.7	A	1028.0	313.34	10.54	18.6			6.26E-05	278	-52.7	T	D	sandstone
2	99	2.7	A	1030.0	313.94	12.37	13.1	4.79E-04	4.54E-04	8.65E-05				C	sandstone
2	100	3.1	A	1036.9	316.05	11.58	21.3			9.56E-05	84.9	-52.2	T	D	sandstone
2	101	1.3	A	1040.1	317.02	11.39	20.9	8.92E-04	8.28E-04	4.58E-05	110.2	-44	A	D	sandstone
2	101	3.5	A	1042.3	317.69	11.14	21.7			7.380E-05	*	*	T	D	sandstone
2	101	6.7	A	1045.5	318.67	11.44	21.8	6.02E-04	5.65E-04	7.876E-05	*	*	A	D	sandstone
2	104	1.7	A	1070.8	326.38	10.64	19.02	1.06E-04	1.05E-04	9.582E-06	*	*	A	J	fine-grained sandstone
2	104	1.8	A	1070.9	326.41	10.4	18.45	9.70E-05	9.52E-05	1.221E-05	*	*	T	J	fine-grained sandstone
2	104	7.3	A	1076.4	328.09	10.8	19.54	9.89E-05	9.71E-05	2.619E-05	*	*	A	J	fine-grained sandstone
2	104	7.4	A	1076.5	328.12	10.9	20.47	1.09E-04	1.06E-04	1.723E-05	*	*	T	J	fine-grained sandstone
2	105	7.1	A	1086.1	331.04	10.95	21.93	1.19E-04	1.18E-04	2.839E-05	*	*	A	J	reworked tuff
2	105	7.2	A	1086.2	331.07	10.89	21.6	1.16E-04	1.14E-04	1.714E-05	116.4	-61	T	J	reworked tuff
2	107	9.3	A	1102.9	336.16	10.66	19.34	1.22E-04	1.19E-04	3.906E-05	78.3	-29.4	A	J	fine-grained sandstone
2	107	9.5	A	1103.1	336.23	10.8	19.86	1.22E-04	1.19E-04	1.559E-05	*	*	T	J	fine-grained sandstone
2	109	2.1	A	1116.0	340.16	10.81	18.86	1.05E-04	1.05E-04	2.486E-05	41.4	-39.4	A	J	reworked tuff

Table 1. Paleomagnetic data, CCM-1 and CCM-2

CORE	RUN	SAMPLE	SUB	Depth,ft	Depth,m	Volume	Mass	LFMS	HFMS	J	D	I	DM	IN	Lithology
2	109	2.2	A	1116.1	340.19	11.44	20	1.10E-04	1.12E-04	2.249E-05	*	*	T	J	reworked tuff
2	109	5.3	A	1119.2	341.13	11.58	19.7	1.32E-04	1.32E-04	2.157E-05	*	*	T	J	reworked tuff
2	109	5.4	A	1119.3	341.16	10.3	16.08	1.14E-04	1.12E-04	2.546E-05	24.9	-41.8	A	J	reworked tuff
2	109	8.3	A	1122.2	342.05	10.58	18.2	1.34E-04	1.30E-04	5.953E-05	22.9	-41	A	J	reworked tuff
2	109	8.4	A	1122.3	342.08	11.24	19.7	1.45E-04	1.42E-04	1.794E-05	*	*	T	J	sandy reworked tuff
2	110	0.7	A	1124.9	342.87	11.53	20	1.60E-04	1.57E-04	1.578E-05	*	*	T	J	sandy reworked tuff
2	110	0.8	A	1125.0	342.90	10.82	18.81	1.57E-04	1.52E-04	3.506E-05	347.9	-47.2	A	J	sandy reworked tuff
2	110	3.4	A	1127.6	343.69	11.44	19.9	3.18E-04	3.07E-04	4.825E-05	74.3	-29.8	T	J	sandstone
2	110	3.5	A	1127.7	343.72	10.62	18.57	3.26E-04	3.10E-04	9.998E-05	*	*	A	J	sandstone
2	110	5.6	A	1129.8	344.36	11.13	24.56	2.07E-03	2.00E-03	5.903E-04	*	*	A	J	coarse-grained sandstone
2	110	5.75	A	1130.0	344.41	11.63	25	5.45E-04	5.27E-04	5.583E-05	342.8	18.4	T	J	sandstone
2	110	6.6	A	1130.8	344.67	10.69	21.64	4.31E-04	4.17E-04	1.374E-04	343.6	-48.3	A	J	coarse-grained sandstone
2	110	6.75	A	1131.0	344.71	11.58	25.7	5.83E-04	5.63E-04	1.132E-04	274.1	0.6	T	J	coarse-grained sandstone
2	112	0.5	A	1145.1	349.03	10.78	16.45	5.49E-05	5.92E-05	5.903E-06	*	*	A	J	reworked tuff
2	112	0.6	A	1145.2	349.06	12.03	18	5.89E-05	6.66E-05	1.299E-06	*	*	T	J	reworked tuff
2	112	3.5	A	1148.1	349.94	10.57	16.03	4.83E-05	5.27E-05	6.476E-06	333.8	78.9	A	J	reworked tuff
2	112	3.6	A	1148.2	349.97	12.08	17.7	5.35E-05	6.04E-05	3.760E-06	*	*	T	J	reworked tuff
2	112	7.8	A	1152.4	351.25	11.88	17.4	5.45E-05	6.18E-05	2.628E-06	*	*	T	J	reworked tuff
2	112	7.9	A	1152.5	351.28	10.9	16.33	5.27E-05	5.69E-05	8.928E-06	*	*	A	J	reworked tuff
2	113	0.9	A	1155.8	352.29	11.39	17.7	6.81E-05	7.25E-05	3.487E-06	*	*	T	J	reworked tuff
2	113	1	A	1155.9	352.32	10.76	16.65	7.20E-05	7.48E-05	5.382E-06	157.1	-46.2	A	J	reworked tuff
2	113	2.5	A	1157.4	352.78	10.7	16.59	9.60E-05	9.79E-05	6.803E-06	145.7	-53.4	A	J	reworked tuff
2	113	2.6	A	1157.5	352.81	11.54	17.7	1.07E-04	1.10E-04	1.049E-05	*	*	T	J	reworked tuff
2	113	7.95	A	1162.9	354.44	11	16.8	2.40E-04	2.40E-04	1.407E-05	68.1	-45.8	T	J	reworked tuff
2	113	8.1	A	1163.0	354.48	10.7	16.15	3.17E-04	3.15E-04	9.062E-05	*	*	A	J	reworked tuff
2	115	2.4	A	1172.3	357.32	11.04	21.56	1.52E-04	1.48E-04	4.261E-05	108.5	-71.3	A	J	fine-grained sandstone
2	115	2.5	A	1172.4	357.35	10.85	20.96	1.63E-04	1.57E-04	1.986E-05	*	*	T	J	sandstone
2	115	7.65	A	1177.6	358.92	11.24	18	9.79E-05	9.59E-05	3.92E-05				C	reworked tuff
2	116	1.3	A	1181.5	360.12	11.19	19.4	3.05E-04	2.96E-04	8.07E-05				C	reworked tuff
2	116	3.8	A	1184.0	360.88	11.04	18.4	4.17E-04	4.05E-04	1.32E-04				C	reworked tuff
2	118	4.45	A	1205.1	367.30	11.04	19.59	2.26E-04	2.13E-04	6.722E-05	45.7	-62.6	A	J	fine-grained sandstone
2	118	4.65	A'	1205.3	367.36	10.7	19.18	2.31E-04	2.18E-04	3.976E-05	26.8	-60.2	T	J	sandstone
2	119	2.2	A	1213.0	369.72	10.71	17.02	1.55E-04	1.48E-04	2.898E-05	*	*	A	J	fine-grained sandstone
2	119	2.4	A	1213.2	369.78	10.66	18.79	1.63E-04	1.55E-04	2.127E-05	*	*	T	J	fine-grained sandstone
2	119	4.2	A	1215.0	370.33	11.04	21.77	1.42E-04	1.37E-04	5.473E-05	277.4	-11.4	A	J	reworked tuff
2	119	4.3	A	1215.1	370.36	10.6	19.8	1.13E-04	1.11E-04	5.823E-06	*	*	T	J	reworked tuff
2	134	1.75	A	1362.7	415.34	11.04	18.8	1.53E-04	1.48E-04	4.568E-05	53.3	-40.3	A	D	sandstone
2	134	2.9	A	1363.8	415.69	11.04	20.6			2.055E-04	31.5	61.5	T	D	sandstone
2	134	4.7	A	1365.6	416.24	11.14	21.3	7.08E-04	6.86E-04	1.311E-04	157.9	42.9	A	D	sandstone
2	134	7.4	A	1368.3	417.06	11.39	20.3	2.82E-04	2.73E-04	1.03E-04				C	fine-grained sandstone
2	135	4.8	A	1373.7	418.70	10.8	20.7			6.726E-04	287.3	26.3	T	D	fine-grained sandstone
2	135	9.45	A	1378.4	420.12	10.9	17.1	2.56E-03	2.52E-03	8.74E-04				C	sandy reworked tuff
2	136	3.5	A	1382.7	421.45	11.19	17.3	1.76E-03	1.74E-03	4.97E-04				C	sandy reworked tuff

Table 1. Paleomagnetic data, CCM-1 and CCM-2

CORE	RUN	SAMPLE	SUB	Depth,ft	Depth,m	Volume	Mass	LFMS	HFMS	J	D	I	DM	IN	Lithology
2	137	0.2	A	1389.6	423.55	11.09	17.6	6.54E-04	6.49E-04	1.67E-04				C	reworked tuff
2	137	7.7	A	1397.1	425.84	11.24	19.2	1.99E-03	1.97E-03	5.34E-04				C	reworked tuff
2	138	6.25	A	1406.0	428.53	10.9	19.7			3.822E-05	177.7	79	T	D	fine-grained sandstone
2	144	1.75	A	1453.0	442.86	11.29	19.7	1.74E-04	1.70E-04	2.37E-05				C	sandstone
2	159	0.45	A	1598.9	487.33	10.95	21.5	6.69E-04	6.44E-04	2.136E-04	297.4	48.8	A	D	sandstone
2	159	9.5	A	1607.9	490.09	11.23	23	8.65E-05	9.04E-05	1.690E-04	94.6	46.3	A	C	tuff breccia
2	160	8.2	A	1616.8	492.80	11.63	26.2	9.42E-05	9.74E-05	1.71E-03				C	tuff breccia; clast
2	163	5.3	A	1644.7	501.31	11.03	26	2.20E-04	2.24E-04	6.19E-04				C	tuff breccia; clast
2	165	6.4	A	1666.3	507.89	11.33	22.8	2.60E-04	2.64E-04	1.52E-04				C	tuff breccia; clast
2	167	1.2	A	1681.6	512.55	11.43	27.4	1.16E-03	1.16E-03	1.790E-02	144.8	30.4	A	C	tuff breccia; clast
2	168	4.5	A	1695.0	516.64	11.38	25.5	1.19E-03	1.18E-03	9.044E-03	58.9	-29.1	A	D	tuff breccia; clast
2	170	8.3	A	1719.0	523.95	11.48	25.2	6.55E-04	6.54E-04	1.760E-03	104.9	37.9	A	C	tuff breccia
2	175	4.2	A	1765.8	538.22	11.73	27.4	7.08E-03	7.07E-03	1.603E-02	21.4	-27.8	A	D	tuff breccia; clast
2	177	9.2	A	1790.8	545.84	12.12	26.7	3.73E-03	3.72E-03	2.020E-03	107.7	-80.7	A	C	tuff breccia
2	178	9.6	A	1800.7	548.85	11.68	24.7	7.29E-03	7.12E-03	2.38E-02				C	tuff breccia
2	180	7.7	A	1819.4	554.55	12.12	24.8	6.85E-03	6.78E-03	1.85E-03				C	sandstone
2	183	0.9	A	1839.9	560.80	11.68	22.4	8.95E-04	8.90E-04	2.11E-04				C	reworked tuff
2	189	3.5	A	1863.3	567.93	11.53	23.9	3.71E-03	3.67E-03	2.777E-03	17	32.1	A	D	breccia
2	191	6.5	A	1886.6	575.04	11.19	22.7	3.53E-04	3.30E-04	2.530E-02	248.7	-12	A	C	tuff breccia; clast
2	193	4.4	A	1904.9	580.61	11.33	24.7	3.13E-03	3.07E-03	1.596E-02	98.5	-52.4	A	D	tuff breccia
2	195	8.9	A	1929.4	588.08	11.23	22.1	3.34E-03	3.22E-03	1.690E-02	313.5	-22.2	A	C	tuff breccia
2	197	2.5	A	1943.0	592.23	11.97	23.3	1.45E-02	1.44E-02	2.810E-03	309.5	61.8	A	D	tuff breccia
2	199	0.4	A	1961.6	597.90	11.09	23.5	5.67E-03	5.61E-03	7.740E-04	140.7	85.6	A	D	fine-grained sandstone
2	199	8.1	A	1969.3	600.24	10.94	22.2			1.381E-03	*	*	T	D	tuff breccia
2	200	1.4	A	1971.5	600.91	11.53	21.2	6.42E-04	6.32E-04	1.05E-04				C	fine-grained sandstone
2	201	0.7	A	1980.7	603.72	11.78	27.9	5.57E-03	5.56E-03	1.01E-03				C	tuff breccia
2	201	7.8	A	1987.8	605.88	11.33	26.9	6.18E-03	6.16E-03	2.370E-03	298	39.3	A	C	tuff breccia
2	202	3.8	A	1994.1	607.80	11.43	25.6	5.92E-03	5.88E-03	1.14E-03				C	tuff breccia
2	203	0.4	A	2000.5	609.75	11.04	21.6	3.17E-03	3.14E-03	9.773E-04	119.3	60.7	A	D	reworked tuff
2	203	2.2	A	2002.3	610.30	11.19	19.7	2.54E-03	2.51E-03	6.231E-04	107.9	61.4	A	D	fine-grained sandstone
2	203	9.1	A	2009.2	612.41	11.06	19.6	4.33E-03	4.28E-03	1.197E-03	45.8	66.8	A	D	fine-grained sandstone
2	205	1.5	A	2022.2	616.37	11.09	19.9	1.34E-02	1.32E-02	6.370E-04	259	68.4	A	D	sandstone
2	206	2.7	A	2033.5	619.81	11.34	19.1	1.98E-02	1.95E-02	3.215E-03	268.3	64.2	A	D	sandstone
2	206	5.4	A	2036.2	620.63	11.39	20.6	2.70E-02	2.64E-02	4.343E-03	292.1	60.9	A	D	sandstone
2	206	6.6	A	2037.4	621.00	11.04	22	3.84E-02	3.75E-02	4.421E-03	162.2	58.2	A	D	coarse-grained sandstone
2	206	7.2	A	2038.0	621.18	11	24	1.16E-02	1.15E-02	3.040E-03	345.6	-16.9	A	C	tuff breccia; matrix
2	208	6.7	A	2057.9	627.25	11.44	21	8.81E-03	8.70E-03	3.45E-03				C	tuff breccia; matrix
2	209	6.9	A	2066.5	629.87	11.58	20.7	2.26E-02	2.22E-02	3.380E-03	191.3	-54.4	A	C	tuff breccia; matrix
2	209	7.1	A	2066.7	629.93	11.43	25.1	1.18E-02	1.17E-02	9.300E-03	197.8	-23.4	A	C	tuff breccia; clast
2	212	9.6	A	2092.6	637.83	11	22	2.36E-02	2.34E-02	4.970E-03	164.7	63.2	A	D	tuff breccia
2	212	9.9	A	2092.9	637.92	11.19	23.9	4.46E-02	4.36E-02	1.968E-02	282.5	-3.5	A	D	tuff breccia; clast
2	214	3.4	A	2103.0	641.00	11.44	22.1	3.27E-02	3.26E-02	7.789E-03	282.5	-54.8	A	D	tuff breccia; matrix
2	215	0.4	A	2110.3	643.22	11.63	25	3.09E-03	2.81E-03	4.360E-02	269.5	46.8	A	D	tuff breccia; clast

Table 1. Paleomagnetic data, CCM-1 and CCM-2

CORE	RUN	SAMPLE	SUB	Depth,ft	Depth,m	Volume	Mass	LFMS	HFMS	J	D	I	DM	IN	Lithology
2	215	0.7	A	2110.6	643.31	11.98	23.7	3.23E-03	3.15E-03	3.520E-03	126.1	57.4	A	C	tuff breccia
2	215	6.4	A	2116.3	645.05	11.19	27.1	5.76E-03	5.67E-03	5.329E-03	28	-9.1	A	D	tuff breccia
2	217	0.5	A	2130.1	649.26	11.58	25.9	1.32E-02	1.30E-02	2.210E-03	162.5	-10.1	A	C	tuff breccia
2	217	5.5	A	2135.1	650.78	11.04	22.1	2.34E-02	2.31E-02	1.348E-03	18.5	65.2	A	D	tuff breccia; matrix
2	218	8.05	A	2147.8	654.64	11.49	23	2.81E-02	2.78E-02	9.580E-03	84.3	73.2	A	C	tuff breccia; matrix
2	220	1.3	A	2160.9	658.64	11.49	25.7			2.180E-02	89.6	80.1	A	D,C	ash-flow tuff
2	220	6.6	A	2166.2	660.26	11.23	26.4	2.91E-02	2.89E-02	1.208E-02	56.7	76	A	D	ash-flow tuff
2	222	6.3	A	2186.5	666.45	11.39	27	1.11E-02	1.09E-02	6.266E-03	343.6	75	A	D	ash-flow tuff
2	225	1.4	A	2203.6	671.66	11.54	25.9	2.73E-02	2.68E-02	2.650E-02	256.9	69.5	A	D,C	ash-flow tuff
2	227	4.7	A	2224.6	678.06	11.54	25.3	2.73E-02	2.67E-02	2.983E-02	307.1	72.4	A	D	ash-flow tuff
2	229	7.4	A	2247.3	684.98	11.44	24.2	2.91E-02	2.88E-02	3.240E-02	105.7	79.3	A	D,C	ash-flow tuff
2	231	7.3	A	2267.4	691.10	11.19	23.7	3.32E-02	3.28E-02	3.812E-02	295.3	73	A	D	ash-flow tuff
2	235	1.3	A	2300.6	701.22	11.29	26	3.23E-02	3.16E-02	4.080E-02	328.1	76.1	A	D,C	ash-flow tuff
2	235	10.1	A	2309.4	703.91	11.24	26.5	3.71E-02	3.62E-02	5.038E-02	344.3	73.6	A	D	ash-flow tuff
2	236	4.3	A	2313.8	705.25	11	26.5	1.03E-03	9.72E-04	8.760E-04	355	76.3	A	D,C	ash-flow tuff
2	236	7.4	A	2316.9	706.19	11	24.2	4.96E-04	4.68E-04	5.207E-04	194.1	74.8	A	D	ash-flow tuff

Table 2. Magnetic susceptibility and total sulfur data for selected CCM samples.

CORE	RUN	SAMPLE	SUB	S	LFMS
1	14	2.8	P*	0.37	4.26E-05
1	16	1.5	P*	0.24	4.44E-05
1	34	4.5	P*	1	5.01E-06
1	42	1.8	P*	0.79	7.22E-06
1	45	5.5	P	0.49	1.193E-05
1	46	0.9	P*	0.73	8.23E-06
1	53	6.3	P*	0.37	4.58E-06
1	75	10.4	P	0.58	4.446E-06
1	81	0	P*	0.92	5.80E-06
1	83	1.3	P*	0.87	5.40E-06
1	86	6.9	P*	1	4.33E-06
1	87	1	P*	0.67	5.35E-06
1	93	9.4	P*	1	4.85E-06
1	95	2.8	P*	0.76	4.12E-06
1	98	3.8	P*	0.76	5.36E-06
1	99	5.1	P*	0.66	4.57E-06
1	100	5.2	P	0.42	4.855E-06
1	102	9.25	P	1.11	8.515E-06
1	105	0	P*	0.7	5.20E-06
1	105	7.9	B,P	0.49	4.038E-06
1	106	4.7	P*	0.61	5.57E-06
1	107	6.3	P	0.3	3.797E-06
1	107	7.8	P*	0.74	4.68E-06
1	109	2.4	P	0.45	5.918E-06
1	111	2.9	P	4.1	2.324E-05
1	114	5.65	P	0.01	7.319E-03
1	115	4.6	P	0.04	3.844E-04
1	118	5.85	P	0.08	5.362E-03
1	121	7.6	P	0.07	1.159E-02
1	122	3.3	P	0.01	1.117E-03
1	125	7.1	P*	0.02	6.52E-04
1	129	4.7	P*	0.21	3.83E-04
1	134	0	P*	0.15	6.31E-04
1	139	7.45	P*	0.03	4.09E-05
1	143	2.1	P*	0.02	7.95E-04
1	146	8.2	P*	0.03	6.54E-04
1	148	0.6	P*	0.04	5.56E-04
1	150	5.8	P*	0.02	6.42E-04

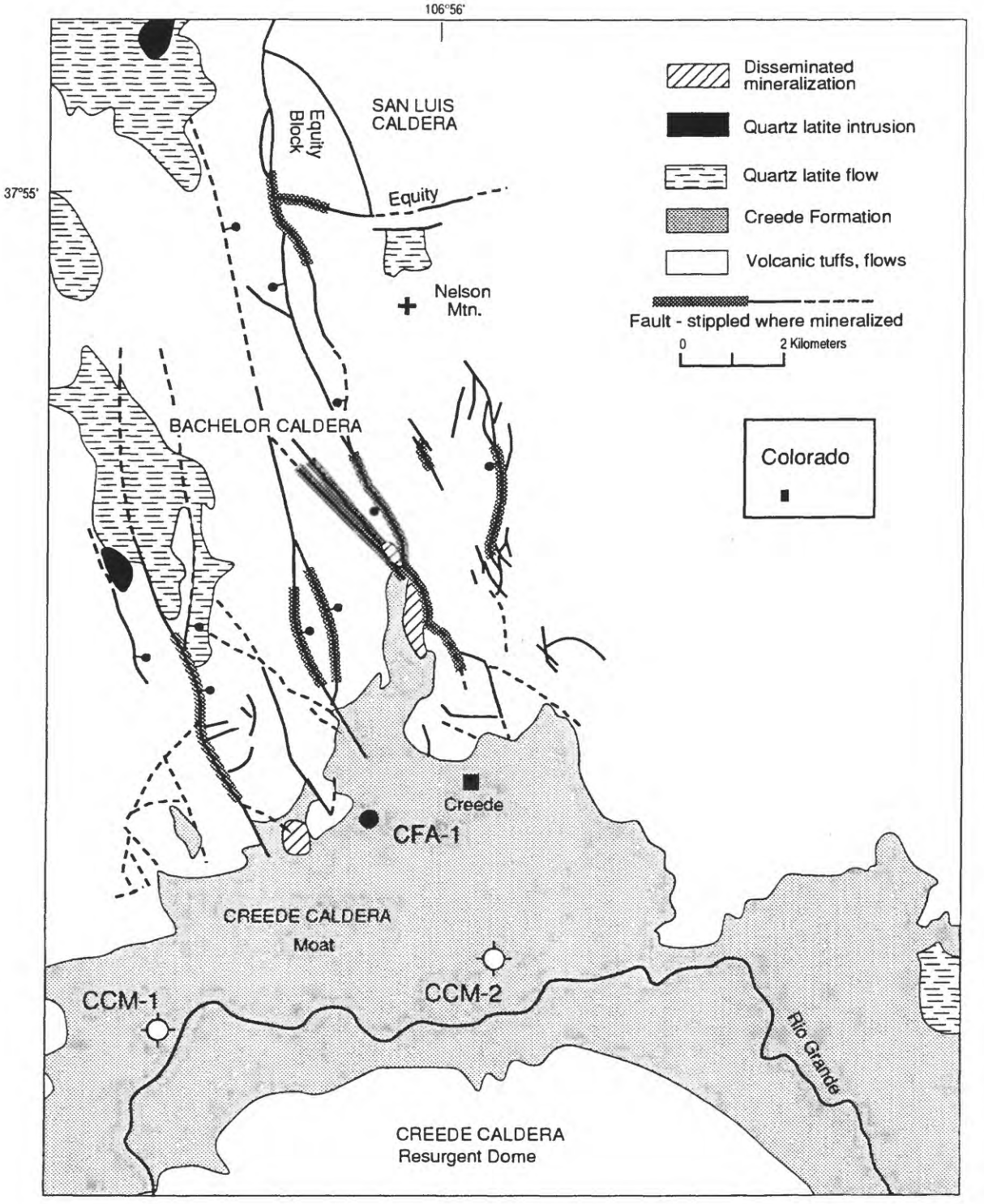

Figure 1. Simplified geologic map (after Steven and Ratte, 1973) of part of the central San Juan volcanic field and the Creede district showing the major structures, mineralized areas, location of air-fall ash site CFA-1, and locations of the CCM-1 and CCM-2 drill holes.

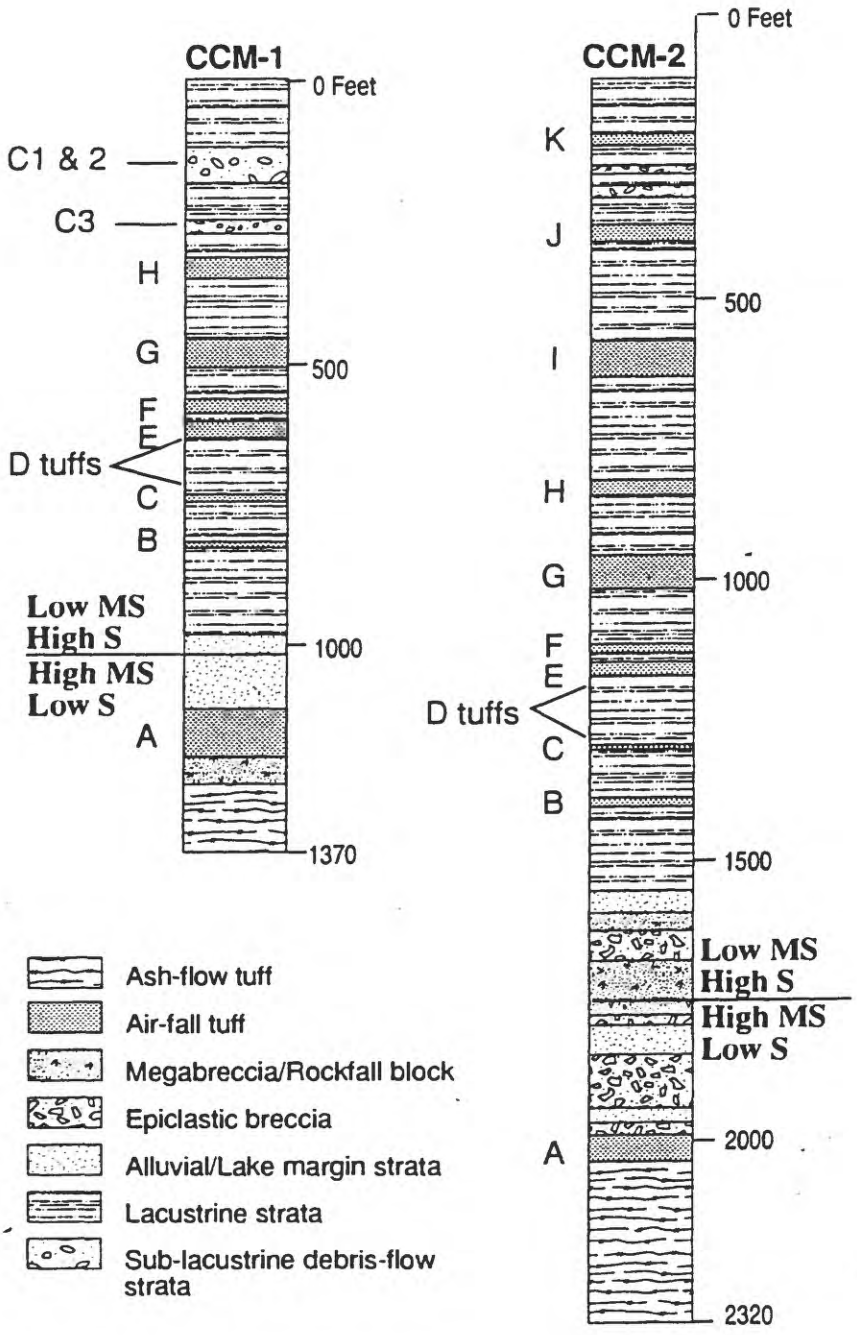

Figure 2. Stratigraphic sections of drill holes CCM-1 and CCM-2 showing major lithic types. Modified from Larsen and Nelson, this volume.

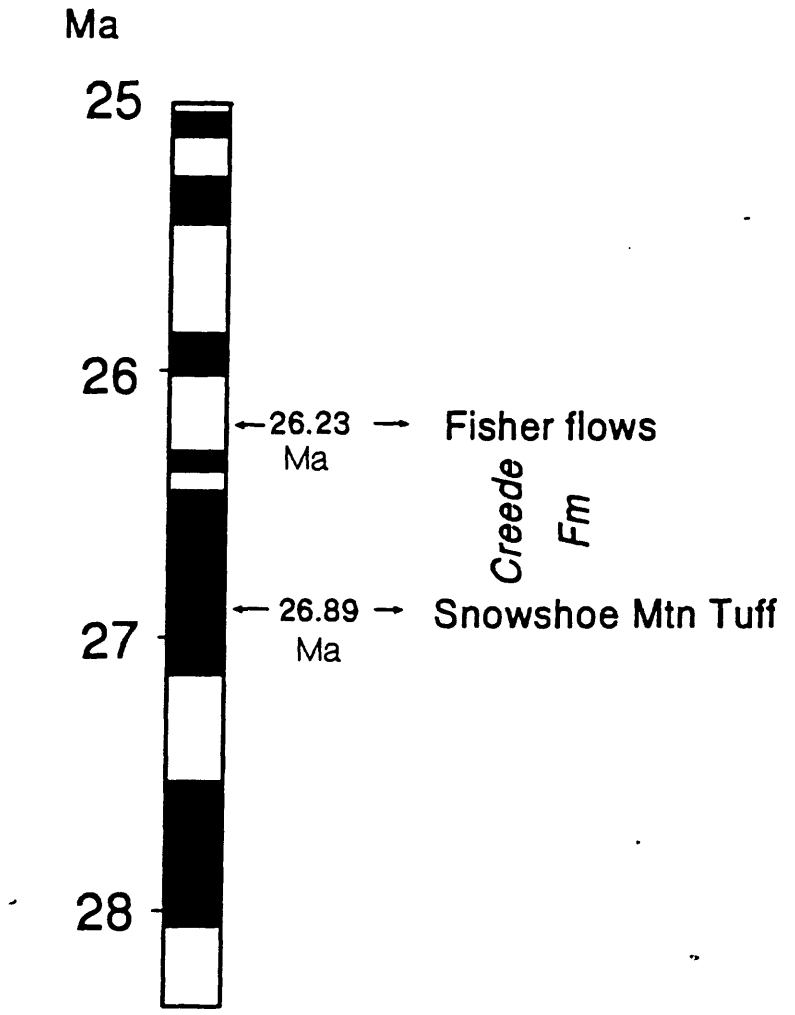

Figure 3. Part of the Oligocene geomagnetic polarity time scale (Harland et al., 1990) with 40Ar/39Ar isotopic dates for volcanic units that bound the sedimentary rocks of the Creede Formation. Each listed date has an uncertainty of +0.05 Ma. The two dated flows are from the upper part of the Fisher Quartz Latite and overlie the Creede Formation. Filled area indicates normal polarity; open area, reversed polarity.

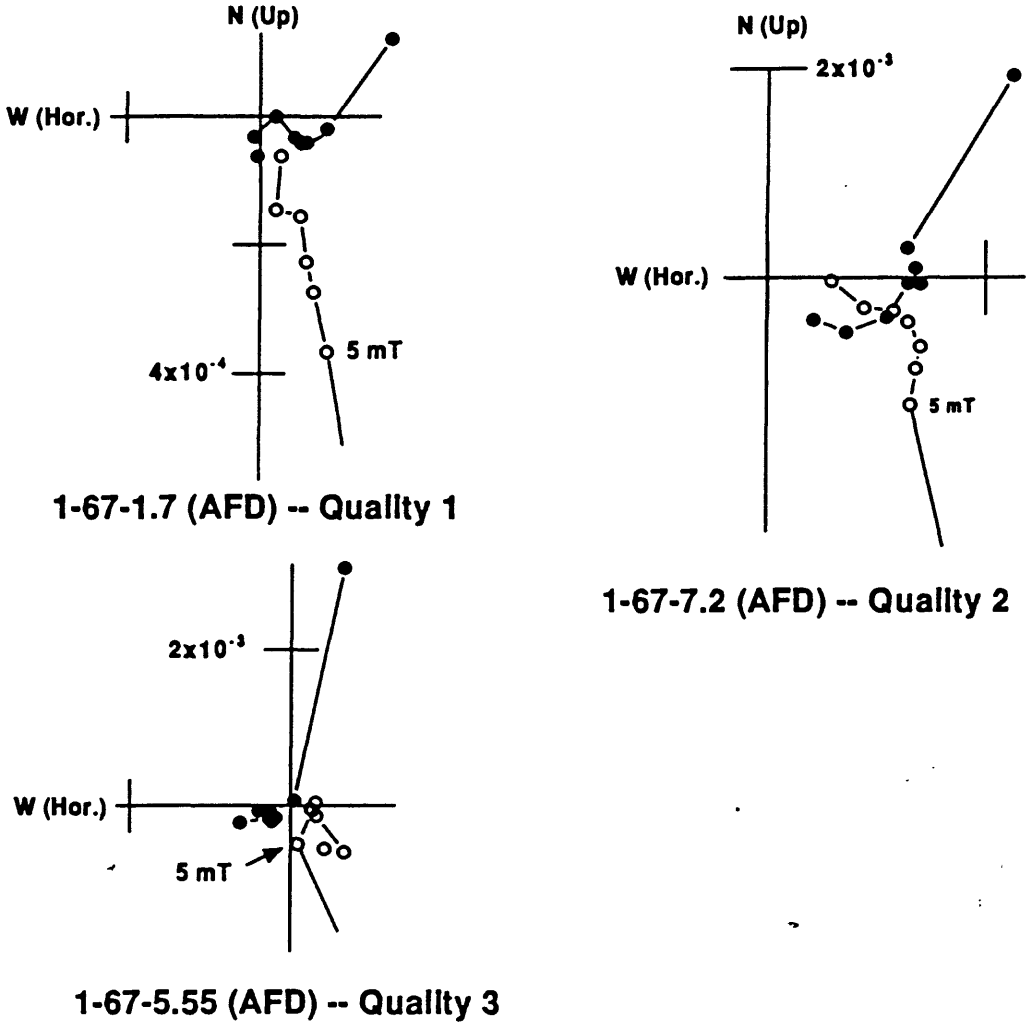

Figure 4. Orthogonal demagnetization diagrams (see Zijderveld, 1967) illustrating three categories of quality of the demagnetization path. Closed (open) symbols represent projections on the magnetic vector on the horizontal (vertical) planes. Remanent magnetizations during AF demagnetization (AFD) are given in Amperes/meter (A/m).

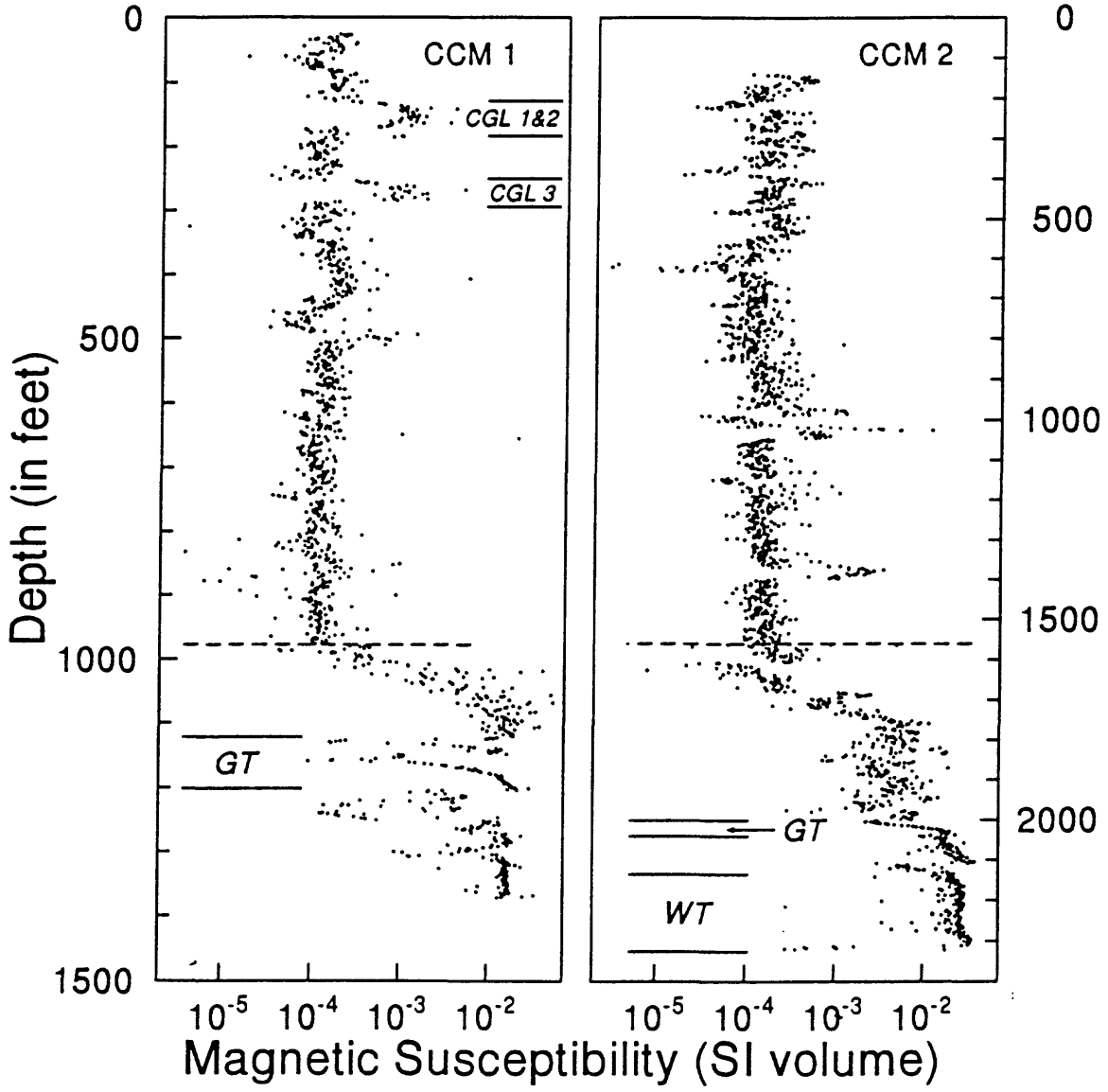

Figure 5. Magnetic susceptibility, from whole-core measurements, plotted against depth in cores CCM-1 and -2. WT=welded tuff; GT=graded tuff; CGL=conglomerate. Only a few lithologic features are illustrated. Dashed line approximates boundary between fluvial facies below and lacustrine facies above.

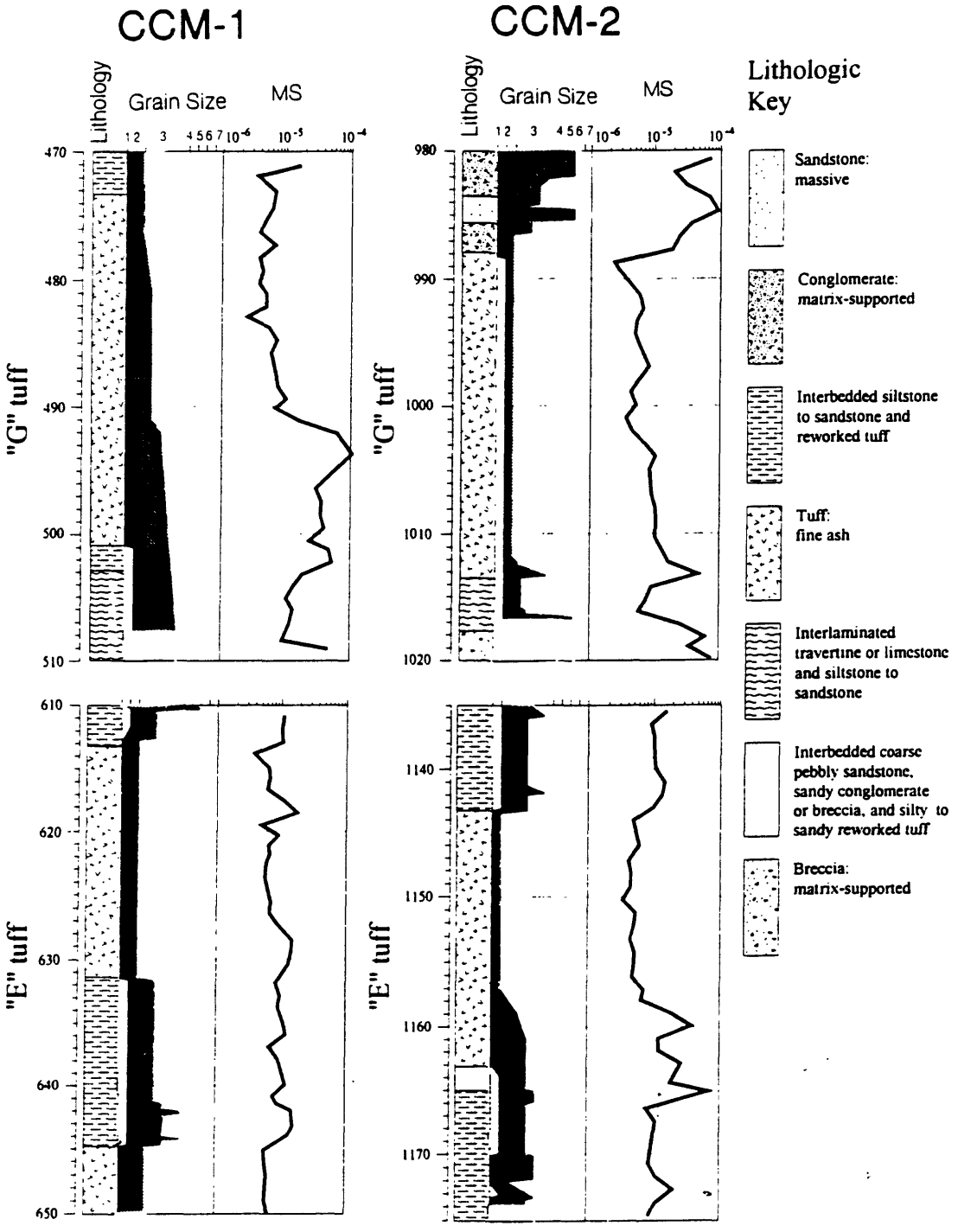

Figure 6. Plots of depth, lithology (Hulen, 1992), grain size (Hulen, 1992), and magnetic susceptibility (MS, in emu/cc) from whole-core pass-through results for selected depths in CCM-1 and CCM-2. Under grain size, 1=clay; 2=silt; 3=sand; 4=granule; 5=pebble; 6=cobble; 7=boulder. A. Plots for G tuffs. B. Plots for E tuffs. G and E tuffs in core CCM-1 are bounded by silty sandstone. G tuff in CCM-2 is bounded above by conglomerate and below by interlaminated limestone and sandstone. E tuff in CCM-2 is bounded above by silty sandstone and reworked tuff and below by interlaminated silty sandstone and sandy siltstone.

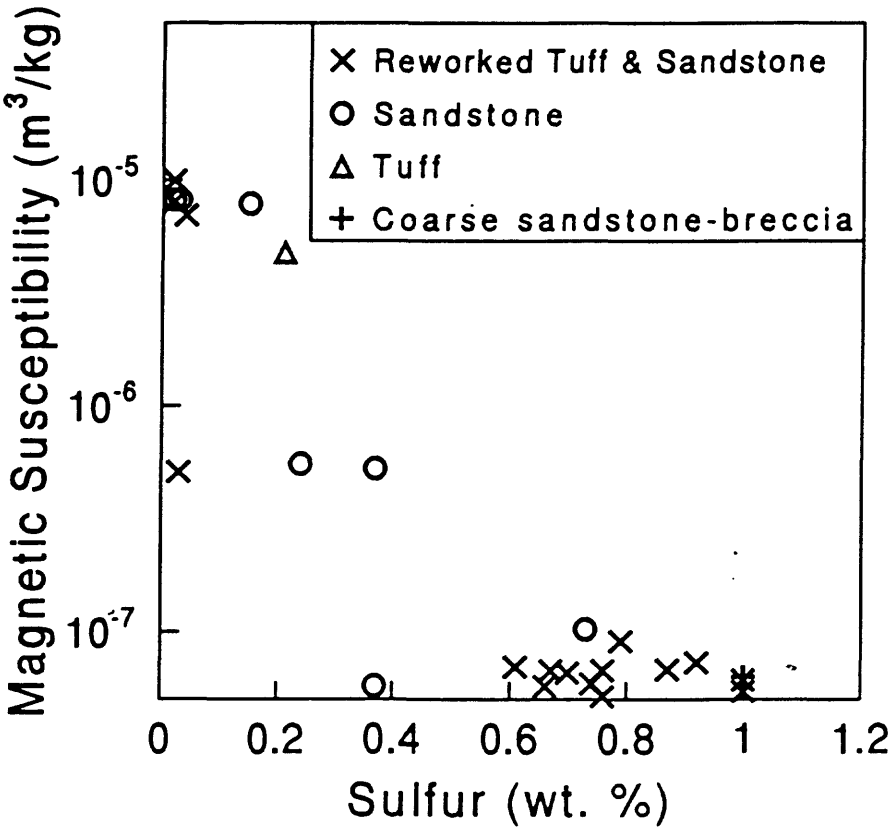

Figure 7. Plot of magnetic susceptibility against total sulfur in individual samples, coded for lithic type.

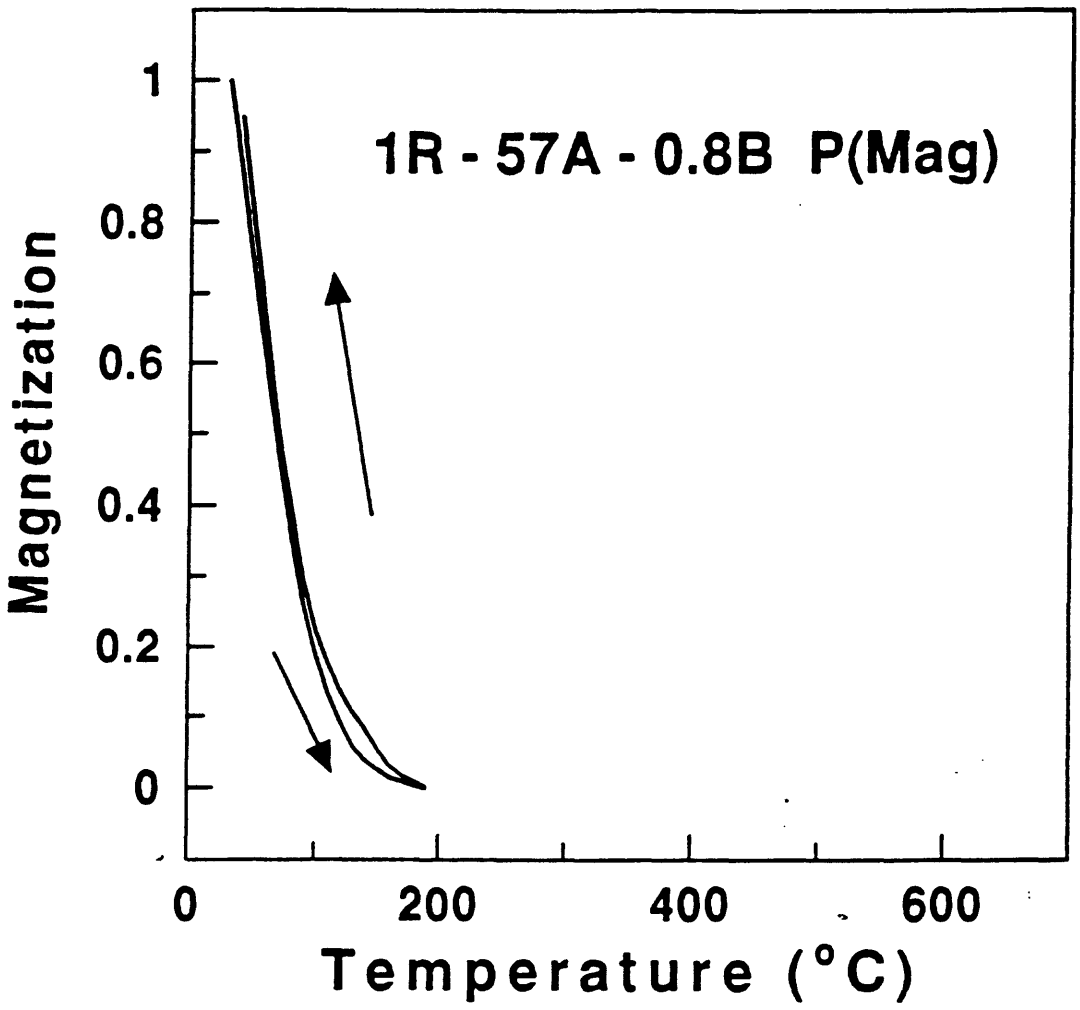

Figure 8. Thermomagnetic curve showing change in normalized magnetization as a function of heating and cooling of magnetic separate from sandstone (sample lR-57A-0.8B; 501.5-ft depth in CCM-l) that contains ferrian ilmenite. The Curie temperature indicated is about 110°C.

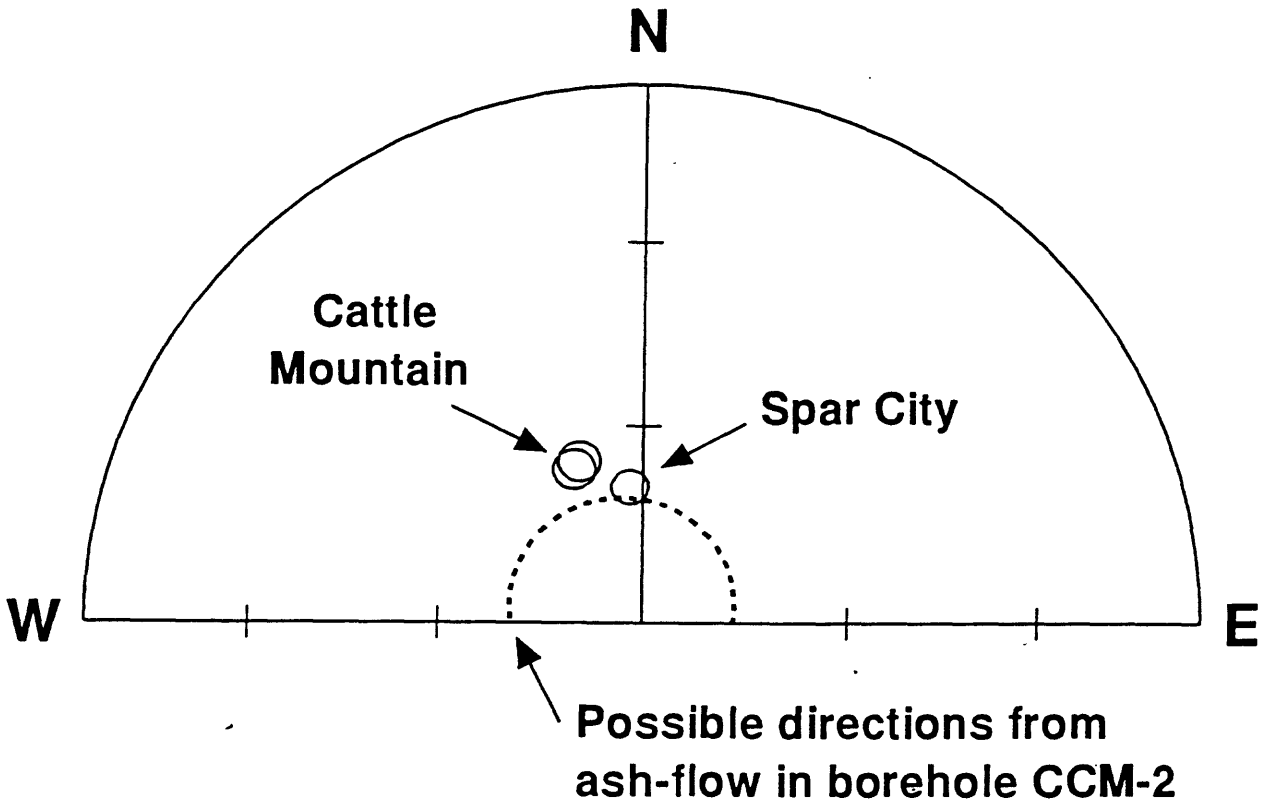

Figure 9. Equal-area stereonet plot of mean inclination of remanent magnetization of the Snowshoe Mountain Tuff at the bottom of core CCM-2. The dashed line represents the possible range in inclination that results from uncertainty in azimuthal orientation combined with the 5° offset in the borehole attitude. All results based on least-squares line fits of the remanent vectors after AF demagnetization. The mean directions of Snowshoe Mountain Tuff from the outcrop sites at Cattle Mountain and Spar City are represented by cones of confidence at the 95% level.

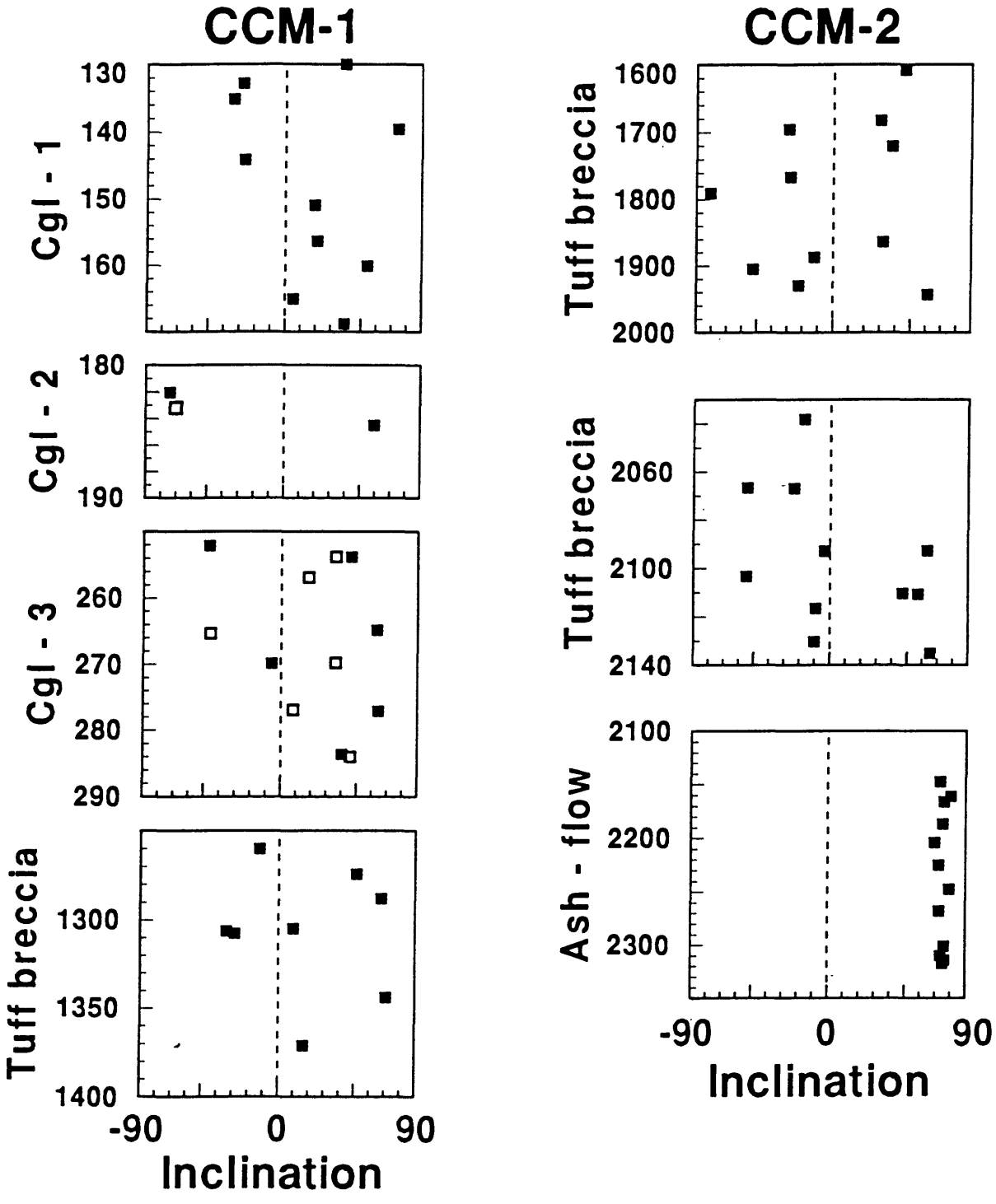

Figure 10. Plots of depth (in feet) against inclination angle, determined by least-squares line fits of the remanent vectors either AF (closed symbols) or thermal (open symbols) demagnetization, for different volcaniclastic lithologies.

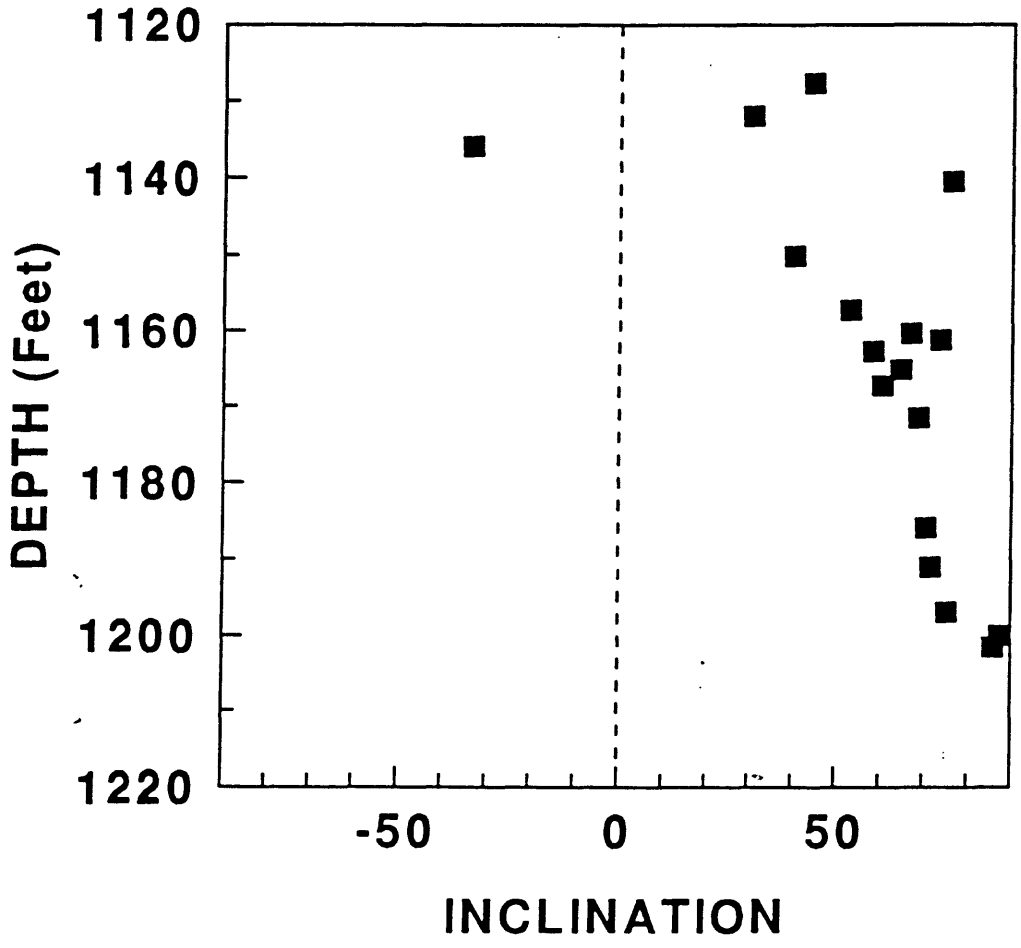

Figure 11. Plot of depth against inclination angle, determined by least-squares line fits of the remanent vectors from AF demagnetization, for graded tuff in core CCM-1.

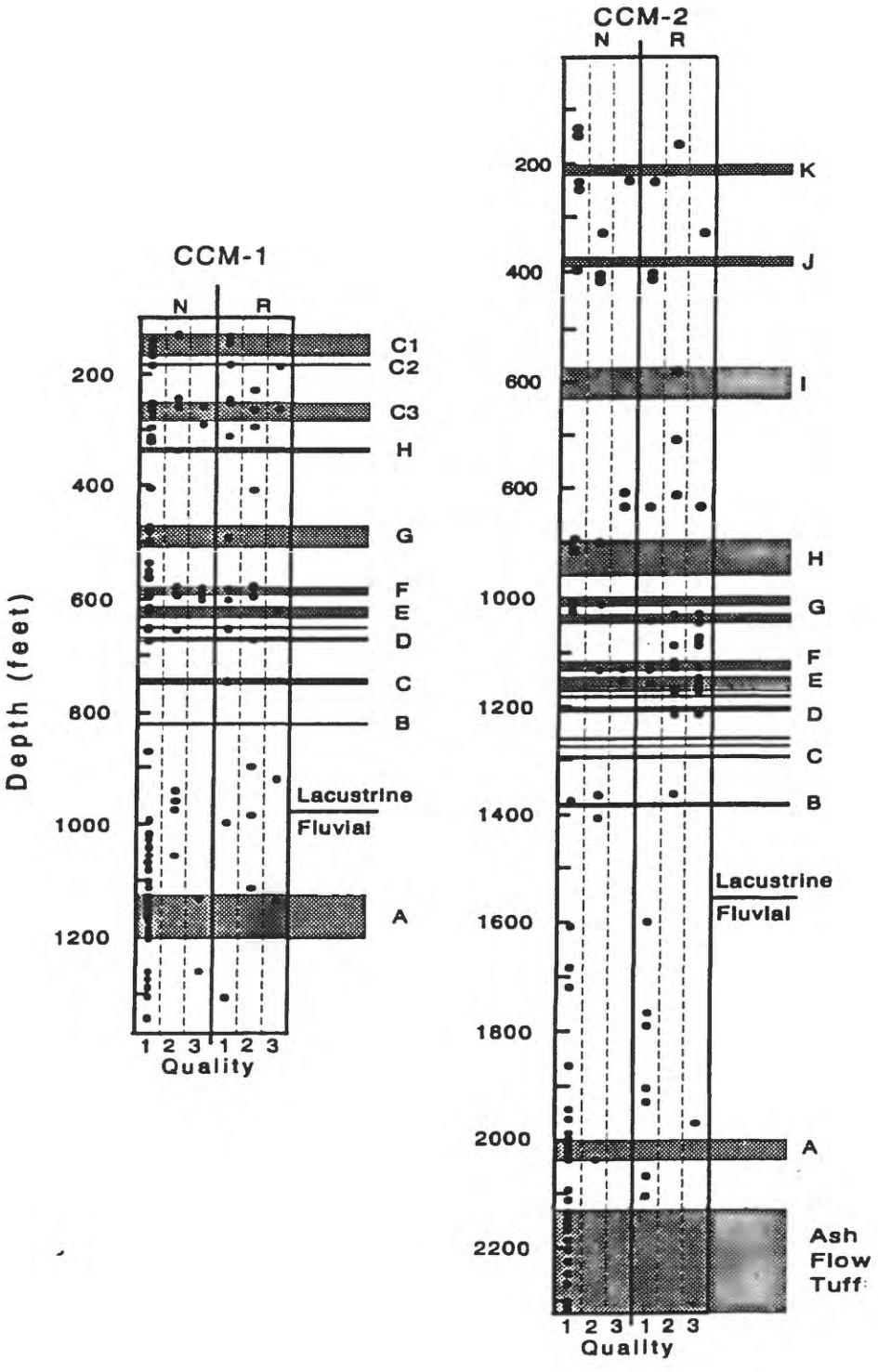

Figure 12. Summary of all paleomagnetic results after AF and thermal demagnetization, cores CCM-1 and CCM-2. Solid circles represent normal (N) or reversed (R) polarity, plotted in columns that represent the quality of the demagnetization path--1, 2, or 3 (see text). Air-fall tuff beds are denoted by letters; C1, C2, and C3 represent conglomerates 1, 2, and 3, respectively. Letters A through K denote air-fall tuff beds.

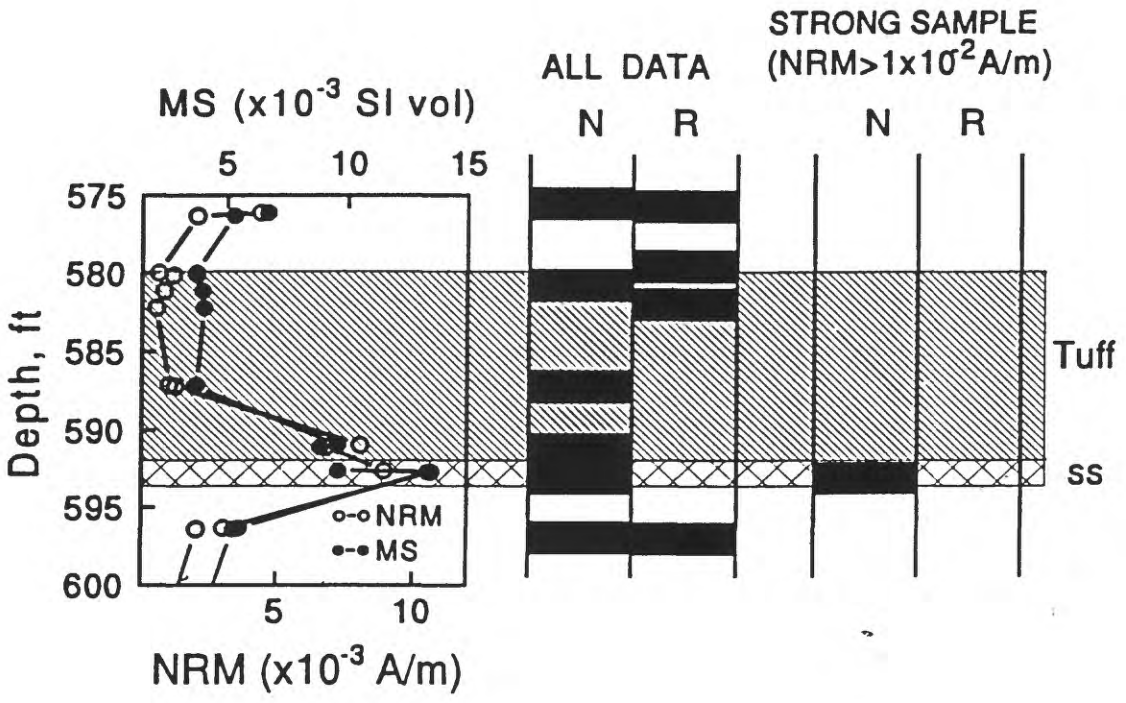

Figure 13. Plot showing variations in magnetic susceptibility (MS) and natural remanent magnetization (NRM) in a tuff bed (F tuff of Larsen and Nelson, this volume), and in enclosing sandstone (cross-hatched) and siltstone (no pattern) in CCM-1. Changes in polarity (N=normal; R=reversed) within the tuff and enclosing beds illustrate complications in polarity stratigraphy.

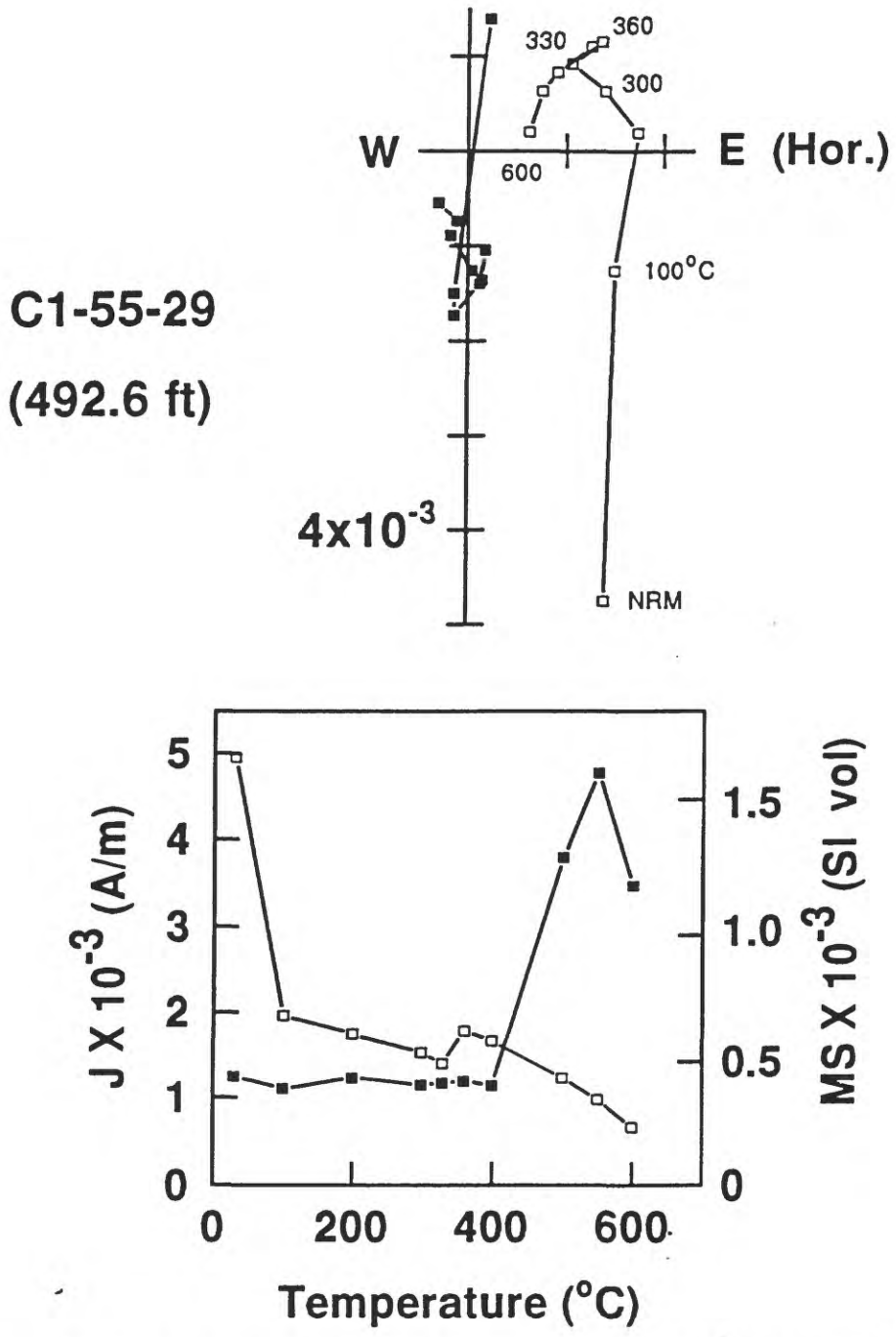

Figure 14. Thermal demagnetization behavior of a specimen of air-fall tuff from core 1, 492.6-ft depth (G tuff of Larsen and Nelson, this volume). The orthogonal demagnetization diagram (upper diagram) shows the removal of the following components: a steep positive-inclination component between NRM and 330 C; a moderate positive-inclination component between 330°C and 360°C; and a moderate to steep negative-inclination component between 360°C and 600°C. Symbols and units as in figure 4. The lower diagram shows a plot of remanent magnitude (open symbols) and magnetic susceptibility (MS; closed symbols) plotted against demagnetization temperature. The increase in MS above 400°C is caused by the alteration of pyrite to magnetite and (or) maghemite).

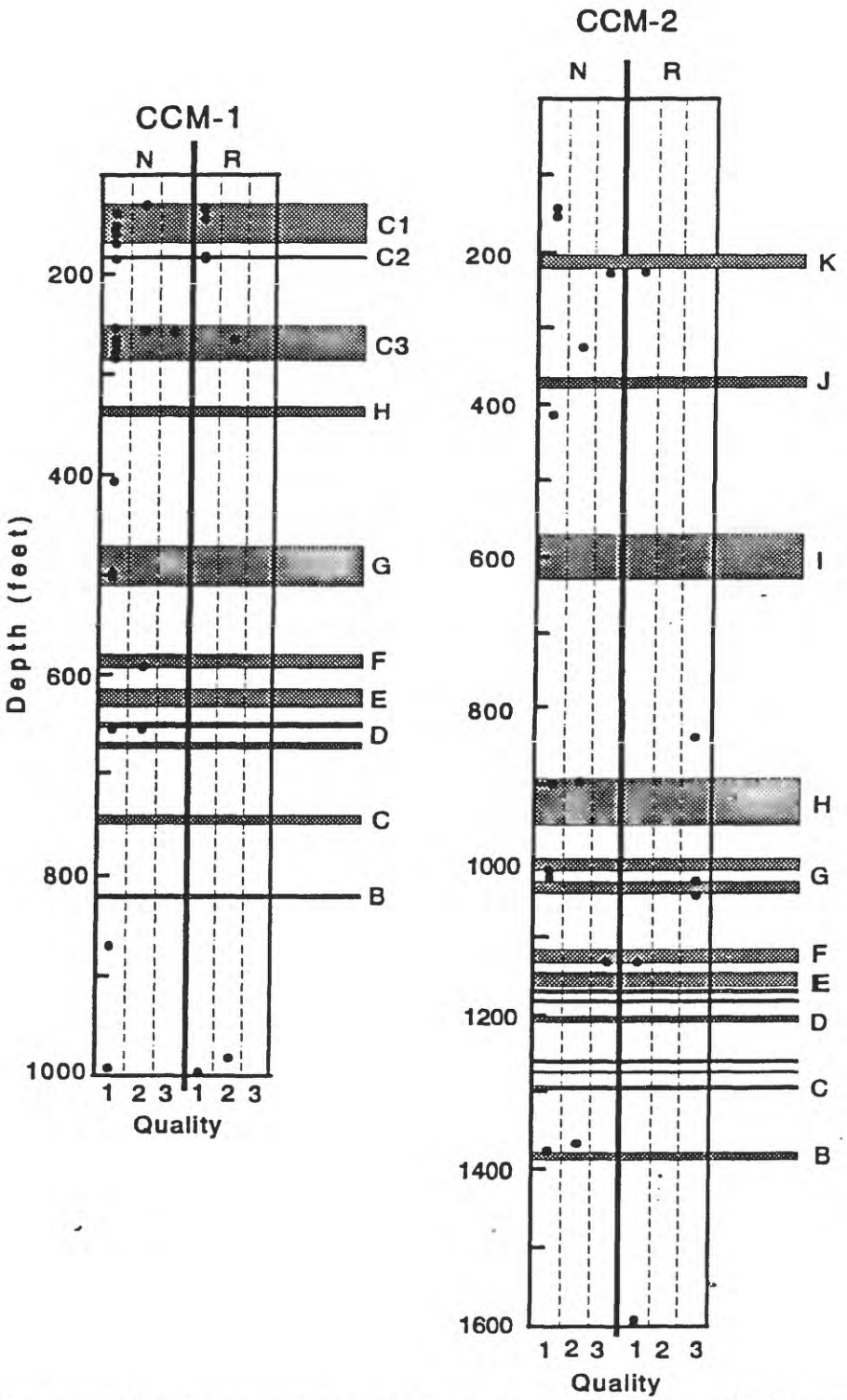

Figure 15. Summary of paleomagnetic results from strongly magnetized (NRM magnitude greater than 10-2 A/m) specimens after AF and thermal demagnetization, cores CCM-l and CCM-2. Solid circles represent normal (N) or reversed (R) polarity, plotted in columns that represent the quality of the demagnetization path--l, 2, or 3 (see text). Air-fall tuff beds are denoted by letters; Cl, C2, and C3 represent conglomerates 1, 2, and 3, respectively. Letters A through K denote air-fall tuff beds.

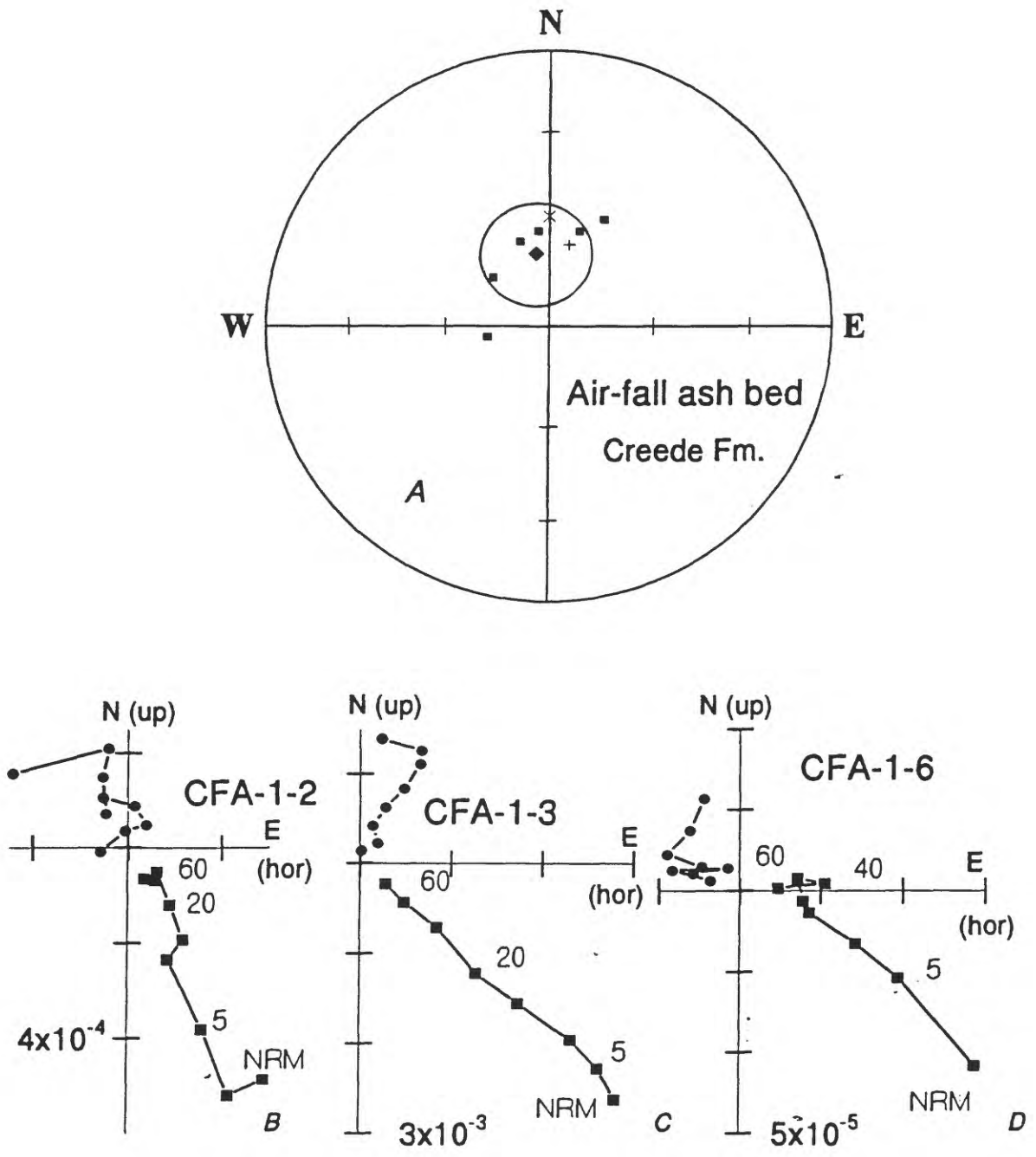

Figure 16. A, equal-area stereonet plot showing directions of remanent magnetization of specimens after AF demagnetization (solid squares), mean direction (solid diamond) surrounded by cone of confidence at the 95% level, expected dipole field direction (x), and present field direction (+). B-D, orthogonal demagnetization diagrams for three specimens, showing range of demagnetization behavior. Magnitudes in A/m. A few demagnetization steps (in mT) are shown.